remote sensing

MDPI

Article

Relationships between Landscape Patterns and Hydrological Processes in the Subtropical Monsoon Climate Zone of Southeastern China

Chong Wei [1,2], Xiaohua Dong [1,2,*,†], Yaoming Ma [3,4,5,6,7,8,†], Menghui Leng [1,2], Wenyi Zhao [1,2], Chengyan Zhang [1,2], Dan Yu [1,2] and Bob Su [9]

1 College of Hydraulic & Environmental Engineering, China Three Gorges University, Yichang 443002, China
2 Engineering Research Center for the Ecological Environment of the Three Gorges Reservoir Area, Ministry of Education, Yichang 430072, China
3 State Key Laboratory of Tibetan Plateau Earth System, Environment and Resources (TPESER), Institute of Tibetan Plateau Research, Chinese Academy of Sciences, Beijing 100101, China
4 College of Earth and Planetary Sciences, University of Chinese Academy of Sciences, Beijing 100049, China
5 College of Atmospheric Science, Lanzhou University, Lanzhou 730000, China
6 National Observation and Research Station for Qomolongma Special Atmospheric Processes and Environmental Changes, Zhikatsé 858200, China
7 Kathmandu Center of Research and Education, Chinese Academy of Sciences, Beijing 100101, China
8 China-Pakistan Joint Research Center on Earth Sciences, Chinese Academy of Sciences, Islamabad 45320, Pakistan
9 Faculty of Geo-Information Science and Earth Observation, University of Twente, 7500 AE Enschede, The Netherlands
* Correspondence: xhdong@ctgu.edu.cn
† These authors contributed equally to this work.

Abstract: With rapid economic development, extensive human activity has changed landscape patterns (LPs) dramatically, which has further influenced hydrological processes. However, the effects of LPs changes on hydrological processes, especially for the streamflow–sediment relationship in the subtropical monsoon climate zone, have not been reported. In our study, 10 watersheds with different sizes in the subtropical monsoon climate zone of southeastern China were chosen as the study area, and the effect of the 14 most commonly used landscape metrics (LMs) on 4 typical hydrological indices (water yields (WY), the runoff coefficient (RC), the soil erosion modulus (SEM), and the suspended sediment concentration (SSC)) were analyzed based on land use maps and hydrological data from 1990 to 2019. The results reveal that the LP characteristics within the study area have changed significantly. The number of patches and landscape shape indices were significantly positively correlated with watershed size ($p < 0.01$). For most watersheds, the largest patch index was negatively correlated with WY, RC, and SEM, and the perimeter area fractal dimension was positively correlated with WY, RC, SEM, and SSC. The effects of several LMs on the hydrological indices had scale effects. WY/RC and the interspersion and juxtaposition index were negatively correlated in most larger watersheds but were positively correlated in most smaller watersheds. Similar results were found for Shannon's diversity/evenness index and SEM. In general, an increase in a small patch of landscape and in landscape diversity would increase WY, the fragmentation of LPs would result in more soil erosion, and LPs would affect the relationship between streamflow and sediment yield. As a result, a proper decrease in landscape fragmentation and physical connectivity in the subtropical monsoon climate zone of southeastern China would benefit soil erosion prevention. These results enhance the knowledge about the relationship between LPs and hydrological processes in the subtropical monsoon climate zone of southeastern China and benefit local water and soil conservation efforts.

Keywords: landscape pattern; runoff coefficient; soil erosion modulus; suspended sediment concentration; subtropical monsoon climate zone; southeastern China

Citation: Wei, C.; Dong, X.; Ma, Y.; Leng, M.; Zhao, W.; Zhang, C.; Yu, D.; Su, B. Relationships between Landscape Patterns and Hydrological Processes in the Subtropical Monsoon Climate Zone of Southeastern China. *Remote Sens.* **2023**, *15*, 2290. https://doi.org/10.3390/rs15092290

Academic Editor: Konstantinos X. Soulis

Received: 6 March 2023
Revised: 18 April 2023
Accepted: 25 April 2023
Published: 26 April 2023

1. Introduction

With the rapid development of human society, land use has changed dramatically [1], which has altered ecosystem structures, functions, and services [2], further influencing eco-hydrological processes [3,4]. The characteristics of land use changes mainly contain land use quantity and landscape patterns (LPs). Scholars have investigated the differences in hydrological effects for various land uses [5–8] to better determine a proper quantity for each land use type for these study regions. Afterward, some scholars further explored the evolution of land use spatial distribution based on various land use prediction models such as the CLUE-S [9], CA [10], and FLUS [11] models. In addition, the spatial distribution and configuration of various land use types could also affect hydrological processes, even with the same quantity. In recent decades, more and more scholars have focused on the effect of LPs on hydrological processes such as runoff and soil erosion [12–14].

LPs are the spatial configuration characteristics of various landscape units with different sizes and shapes [15]. Various landscape metrics (LMs) have been developed to describe the characteristics of LPs [16–18]. Over recent decades, scholars have indicated that LPs have significant correlations with runoff [12], soil erosion [13,14], water quality [19,20], and organic matter decomposition [21,22]. Sadeghi et al. [23] investigated the relationships between LMs and hydrographic components within the Galazchai watershed in Iran. The results show that the number of disjunct core areas (NDCA) was positively correlated with flood volume, and patch density (PD) was positively correlated with peak discharge. Zhao and Huang [24] examined the effects of LPs on runoff within a small watershed in southern China. The results indicate that PD and landscape shape index (LSI) were negatively correlated with runoff, whereas Shannon's diversity index (SHDI) and the landscape division index (DIVISION) were positively correlated with runoff. In addition, PD, SHDI, and largest patch index (LPI) had the largest impacts on variations in runoff. Zhang et al. [25] attempted to reveal the effect of changes in LPs on soil erosion in a small watershed. The results suggest that soil erosion was positively correlated with the patch cohesion index (COHESION) but negatively correlated with LPI, modified Simpson's evenness index (MSIEI), and aggregation index (AI). Another study conducted on the island of Crete in Greece [26] found that there was a significant correlation between average soil erosion and PD, edge density (ED), LPI, and percentage of landscape (PLAND). The topic of the effects of LPs variations on various hydrological processes has been a research hotspot over the last decade.

The most popular methods used to investigate the relationships between LPs and hydrological processes are various correlation analysis (the correlation coefficient method [27], stepwise regression analysis [28], multiple linear regression [25], etc.) methods. In addition, hydrological series have mainly been simulated using multiple hydrological or soil erosion models such as the SWAT [29], InVEST [30], IUH [23], RUSLE [26], WaTEM/SEDEM [31] models with various land use maps as inputs, which are further used for analysis with LMs calculated from the corresponding land use maps. The number of land use maps ranges from 3 to 8 in the previously mentioned works, which is insufficient and possibly brought uncertainty into the results. In addition, most of them used simulated hydrological series from multiple eco-hydrological models that ignored the effect of different LPs on hydrological processes. For instance, the SWAT model separates the watershed into several sub-watersheds and further divides them into more hydrological response units (HRUs) based on different combinations of land use, soil, and slope belt [32]. The hydrological processes were simulated at an HRU scale and then aggregated into a sub-watershed scale. The SWAT model is used to calculate the runoff and sediment generation based on specific combinations of land use, soil, and slope belt, but it does not consider the effects of LPs on the streamflow convergence process and the sediment transportation process. As reported by previous studies, the impacts of LPs on hydrological processes are mainly concentrated in the streamflow converge process and sediment transportation process [33]. Hence, simulated hydrological processes based on the SWAT model ignore the major effects of LPs on these hydrological processes. The RUSLE model simulates soil erosion using an experience

equation containing six factors [26], which also does not take LPs into consideration. In addition, the simulation results also contain errors compared to the observed data to some extent.

The existing relevant studies mainly focus on specific watersheds all over the world, and the areas of these watersheds range from 16.6 to 320,000 km^2 [17,23,24,26]. As scale is a fundamental concept, analyses at various scales may have resulted in different results or even reverse results [34]. In addition, differences in soil type, topography, and meteorology within various regions could also have been a possible driver for the different results. For example, SHDI was positively correlated with runoff in some regions [17,35] and negatively correlated with runoff in other regions [36,37]; PD was positively correlated with the sediment yields load (SYL) in some regions [34,38] and negatively correlated with SYL in other regions [35,36]. Similar reverse results were also observed for COHESION, LPI, SHEI, AI, CONTAG, LSI, etc. in various regions [25,31,33,39]. These phenomena may suggest that it is insufficient to reveal the relationships between LPs and hydrological processes using relevant data from only one watershed. To investigate the impacts of LPs on water quality across Taiwan, Chiang et al. [40] revealed relationships between 12 water quality parameters and 12 LMs based on water quality records for 10 watersheds. The results show that temperature, PH, NO_3-N, and TN are significantly correlated with most LMs in these watersheds. A similar relevant study has not been reported to have been conducted for runoff/SYL and LMs. In addition, the relationship between LMs and suspended sediment concentration (SSC) has not been reported until now. As SSC is an important hydrological index that could reflect the relationship between streamflow and suspended sediment in a watershed, understanding the driving factors behind SSC would benefit not only soil erosion prevention, but also the prevention and control of river reservoir siltation. As the existing studies report, LPs influence runoff and SYL, mainly during the transportation process. It is necessary to conduct a relevant study to investigate whether LPs changes affect SSC to better understand the driving factors behind SSC.

In previous studies, scholars investigated the relationships between LPs and hydrological processes in specific watersheds, but relevant studies focused on climate zones are still rare. Soil erosion brought by rainfall and runoff is strongly controlled by climate [41], and it is important to investigate the effects of LPs on hydrological processes in various climate zones. The subtropical monsoon climate zone is characterized by high annual rainfall and concentrated summer rainfall, which would result in severe soil erosion [42]. The subtropical monsoon climate zone covers ~29% of China's total area, is mainly distributed in southeastern China, and has experienced rapid economic development and land use changes. In addition, southeastern China contains a variety of landforms and shows a general conversion from mountains and hills to plains from south to north, which are more likely to suffer soil erosion. As pronounced by the Resource and Environment Science and Data Center, Chinese Academy of Sciences (RESDC), ~56.39% of Chinese land suffers from water erosion, with this percentage accounting for almost all of southeastern China [43]. However, how LPs changes affect hydrological processes within the subtropical monsoon climate zone of southeastern China is still unclear. Under the background of global climate change and land use change resulting from extensive human activity, it is significant to reveal the relationships between LPs and representative hydrological processes for better land use management for water and soil conservation. To settle this issue, 10 watersheds with area ranging from 1700 to 80,900 km^2 were chosen as the study area, and water yields (WY), runoff coefficient (RC), soil erosion modulus (SEM), and SSC were chosen as the representative hydrological indices to determine the correlations between the chosen hydrological indices and the most studied LMs from 1990 to 2019 in the subtropical monsoon climate zone of southeastern China. The results enhance the knowledge about the effects of LPs on hydrological processes in the subtropical monsoon climate zone of southeastern China for better land use management with an objective of soil and water conservation.

2. Study Area

A total of 10 watersheds (Zhuji (ZJ), Dufengkeng (DFK), Hushan (HS), Lijiadu (LJD), Lanxi (LX), Boluo (BL), Chaoan (CA), Shijiao (SJ), Zhuqi (ZQ), and Waizhou (WZ)) of different sizes in southeastern China, which were dominated by the subtropical monsoon climate, were chosen as the study area (Figure 1). The study area covered a region between 112.1°~120.7°E, and 22.5°~30.0°N, which is mainly dominated by hills and mountainous terrain, with its highest elevation being 2191 masl and its lowest elevation being −136 masl. The main climatological characteristics in the subtropical monsoon climate zone are temperature and precipitation, which are higher in the summer and lower in the winter, and annual precipitation, which is high but unevenly distributed throughout the year. The annual average temperature and precipitation in southeastern China range from 15 to 22 °C and from 1500 to 2200 mm, respectively. The region is rich with river networks and has a developed water system, which is mainly replenished by precipitation. The main geographical and hydrological characteristics of the chosen watersheds are shown in Table 1. The dominant land use of the study area is forest and agricultural land, and LPs have changed rapidly in the last 30 years due to intensive human activity. The main LP changes were an expansion of urban land and water areas and a reduction in forest and agricultural land from 1990 to 2019.

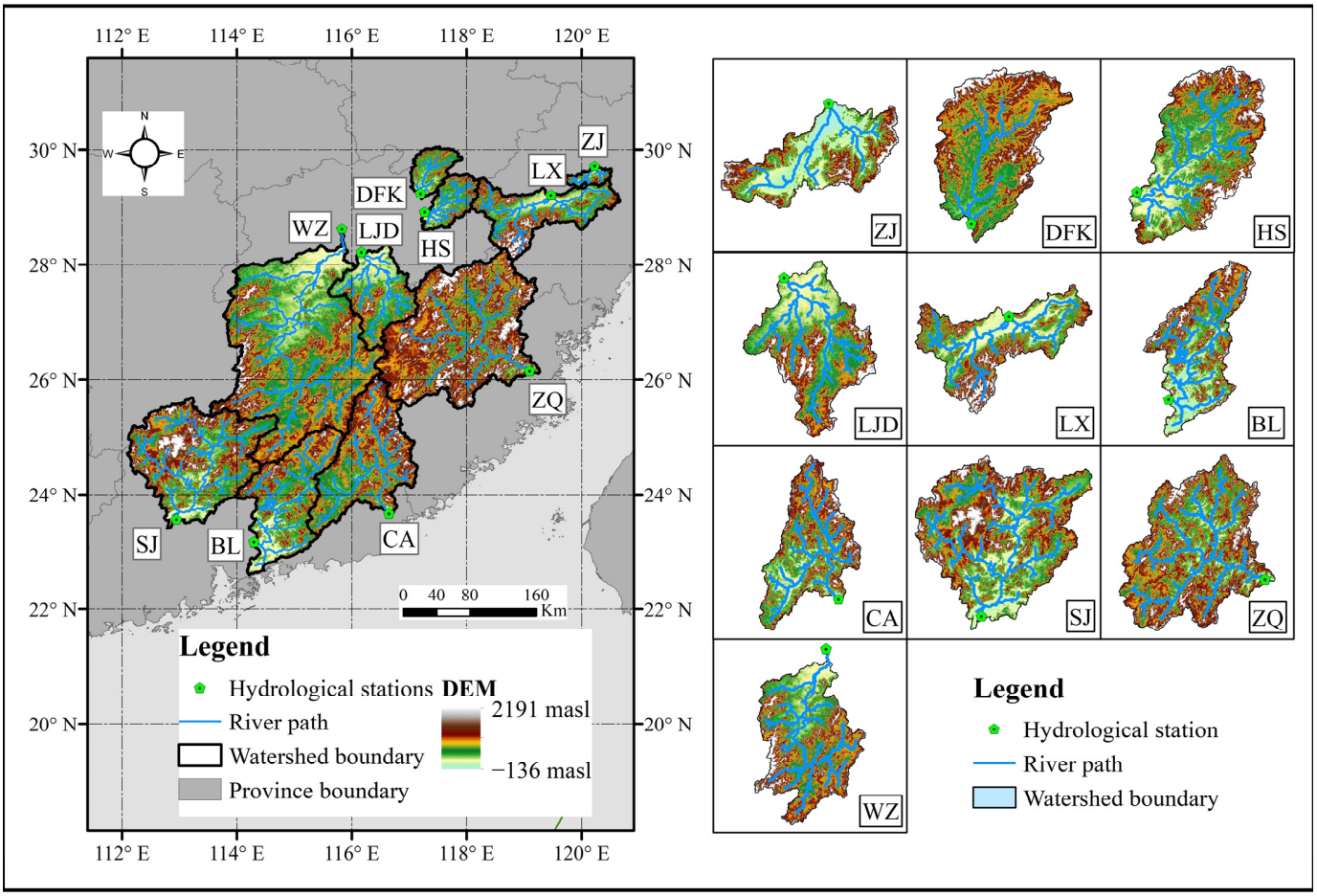

Figure 1. The distribution of the study regions. "ZJ", "DFK", "HS", "LJD", "LX", "BL", "CA", "SJ", "ZQ", and "QZ" represent the "Zhuji", "Dufengkeng", "Hushan", "Lijiadu", "Lanxi", "Boluo", "Chaoan", "Shijiao", "Zhuqi", and "Waizhou" watersheds, respectively.

Table 1. Hydrological and geographical characteristics of the chosen watersheds from 1990 to 2021.

Stations	DA (km^2)	AE (m)	PRE (mm)	WY (10^8 m^3)	RC	SYL (10^4 t)	SEM (t/km^2)	SSC (mg/L)
ZJ	1700	232	1686	12.17	0.41	8.90	52.38	0.07
DFK	5000	243	2054	50.44	0.48	52.97	105.94	0.09
HS	6400	255	2162	71.01	0.52	104.16	162.75	0.13
LJD	15,800	222	2003	124.99	0.39	120.76	76.43	0.09
LX	18,200	352	1942	180.89	0.50	232.69	127.85	0.12
BL	25,300	288	2006	222.21	0.44	131.96	52.16	0.05
CA	29,100	397	1825	235.32	0.45	321.79	110.58	0.12
SJ	38,400	384	1994	416.69	0.55	463.70	120.75	0.11
ZQ	54,500	533	1982	544.55	0.50	278.93	51.18	0.04
WZ	80,900	300	1812	713.52	0.49	382.66	47.30	0.05

Note: DA, AE, and PRE represent drainage area, average elevation, and precipitation, respectively.

3. Data and Methods

3.1. Data Description

The main data used in this study consist of land use maps, precipitation records, and annual runoff and sediment yield records. The land use maps from 1990 to 2019 were obtained from Wuhan University [44] with a spatial resolution of 30 m. The land use maps were generated using the random forest classifier and the visual interpretation method, and they were validated with three sources of test samples. They divided the land use type into 9 categories: cropland, forest, shrub, grassland, water, snow and ice, barren, imperious, and wetland. They can be obtained at https://zenodo.org/record/4417810 (accessed on 28 December 2022), and they have been employed in many studies [19,45,46]. The precipitation records were obtained from China Scientific Data with a temporal resolution of monthly (1960–2020) and a spatial resolution of 1 km [47]. The precipitation records were interpreted with ANUSPLIN 4.4 based on ~2400 precipitation monitoring stations within China and were validated by comparing them with the precipitation records from precipitation gauges and the Chinese hydrological yearbook. The precipitation records that were used can be downloaded at http://doi.org/10.11922/sciencedb.01607 (accessed on 25 December 2022). The measured annual runoff and sediment yield records from 1990 to 2019 of the DFK, LJD, LX, BL, CA, SJ, ZQ, and WZ watersheds and those from 2002 to 2019 of the ZJ and HS watersheds were obtained from the Bulletin of River Sediment in China and were downloaded at http://www.mwr.gov.cn/sj/tjgb/zghlnsgb/ (accessed on 30 December 2022). The bulletins were compiled jointly by the Department of Hydrology of the Ministry of Water Resources, the Monitoring and Forecasting Center for Hydrology and Water Resources of the Ministry of Water Resources, the International Sediment Research and Training Center, and the hydrology bureaus of the river basin institutions, which are very credible. The annual runoff and sediment yield records were used to represent the historical hydrology conditions within the chosen watersheds.

3.2. LMs Selection

LMs were used to represent the spatial distribution characteristics of the various land use patches, and they have been widely used to investigate the relationships between LPs and eco-hydrological processes [21,25,39,48]. The LMs were divided into three categories based on different levels: patch-level, class-level, and landscape-level metrics [39]. The LMs on a landscape level integrated all patch types or classes over the entire study region, and they were separated into four categories reflecting different types of characteristics of landscapes: edge area, shape, aggregation, and diversity metrics [49]. The main purpose of this study was to reveal the relationships between landscape patterns and representative hydrological indices in the subtropical monsoon climate zone. Hence, 14 widely used LMs, which were found to have different relationships with runoff/sediment in various regions, were chosen for this study [17,25,27,31,33,35,36,38,39,50,51]. The selected LMs were LPI, ED, perimeter area fractal dimension (PAFRAC), number of patches (NP), DIVI-

SION, AI, interspersion and juxtaposition index (IJI), contiguity index (CONTAG), PD, LSI, COHESION, SHDI, Shannon's evenness index (SHEI), and MSIEI. Their definitions and relevant literature are shown in Table A1, and these LMs were calculated using Fragstats v4.2.1 software for all land use maps from 1990 to 2019 for all chosen watersheds. Before calculation, the land use types were reclassified into seven categories: agricultural land, forest land, shrubland, grassland, water area, urban land, and bare land.

3.3. Hydrological Indices

To better evaluate the relationships between hydrological processes and LPs, five fundamental hydrological indices (WY (m^3); RC; SYL (t); SEM (t/km^2); SSC (mg/L)) relevant to runoff, sediment yields, and streamflow–sediment relationships were chosen for the study and obtained on an annual scale. These hydrological indices have been employed in previous studies to investigate the hydrological characteristics of various regions [29,52–55]. In this paper, WY, SYL, and SSC values were collected from the Bulletin of River Sediment in China. RC and SEM were calculated using Equations (1) and (2).

$$RC = \frac{WY}{1000 \cdot DA \cdot PRE} \quad (1)$$

$$SEM = \frac{SYL}{DA} \quad (2)$$

where WY represents annual water yield (m^3); DA represents drainage area (km^2); PRE represents annual precipitation (mm); SYL represents the annual sediment yield load (t).

3.4. Analysis Methods

Linear regression [56] was used to analyze the change trends of various hydrological indices and of LMs from 1990 to 2019 for the chosen watersheds. This type of analysis has been widely employed in previous relevant works and has shown reasonable results [43,57,58]. In addition, the F-test [59] was adopted to test the significance of the trend for each series at confidence levels of 0.05 and 0.01. The equation form of the linear regression is as follows:

$$y = ax + b \quad (3)$$

where y represents the dependent variable (WY, RC, SYL, SEM, and SSC); a represents the change trend per year; x represents year; b represents the constant.

To investigate the exchanges between different land use types from 1990 to 2019, the period was separated into two stages: 1990–2005 and 2005–2019. Land use conversion analysis was conducted for land use maps in 1990, 2005, and 2019 in the ArcGIS 10.2 platform. To better show the exchanges between different land use types, land with no land use type exchanges was ignored when conducting relevant analyses. With this method, the exchanges between each land use type from 1990 to 2019 were analyzed for the chosen watersheds.

The effects of LPs changes that propagate to hydrological processes have lag times that vary according to differences in watershed size, climate, landscape, topography, soil type, etc. [60–62]. In previous studies, lag times of 0–4 years were needed before significant responses of hydrological processes to landscape changes could be observed [63,64]. Hence, a slip correlation analysis [43] was conducted with a lag time of 0–4 years to investigate the relationships between LPs and hydrological indices. A description of the slip correlation analysis is as follows:

(1) The origin series X and Y are: $X(x_1, x_2, \ldots, x_{n-1}, x_n)$; $Y(y_1, y_2, \ldots, y_{n-1}, y_n)$. The X and Y series are the landscape series and hydrological indices, respectively; n is the series number, which corresponds to the year.

(2) The clip correlation series for X and Y were established. For the lag time of i years, the X′ and Y′ series are $X'(x_1, x_2, \ldots, x_{n-i-1}, x_{n-i})$ and $Y'(y_i, y_{i+1}, \ldots, y_{n-1}, y_n)$, respectively. The value of *i* ranges from 0 to 4, and it represents lag times of 0–4 years.

(3) The correlation coefficient (CC_i) between X′ and Y′ was calculated, and the result was the lag correlation between X and Y with a lag time of i years. The highest value of CC_i with a significance of 0.05 was regarded as the lag time between X and Y.

As SEM was calculated by dividing SYL by DA, the SEM series was linearly correlated with SYL and removed the effect of watershed size on soil erosion. In this paper, a slip correlation analysis was conducted between the 14 LMs and 4 hydrological indices (WY, RC, SEM, and SSC) in the chosen watersheds.

4. Results

4.1. Variations in SY, RC, SYL, SEM, and SSC

Table 1 shows the annual average values of various hydrological indices, and Figure 2 shows variations in WY, RC, SYL, SEM, and SSC. The annual average WY, SYL, RC, SEM, and SSC values for the chosen watersheds ranged from 12.17 × 10^8 to 713.52 × 10^8 m^3, from 8.9 × 10^4 to 463.7 × 10^4 t, from 0.39 to 0.55, from 47.3 to 162.75 t/km^2, and from 0.05 to 0.13 mg/L, respectively. The variations in WY were higher within ZQ and WZ, followed by LJD, LX, BL, CA, and SJ, and the variations in SYL were obviously higher within CA, SJ, ZQ, and WZ compared to the other watersheds. In addition, the variations in SEM and SSC were higher within DFK, HS, LX, and CA compared to the other watersheds, which indicates that soil erosion in these watersheds was much more serious compared to the other watersheds.

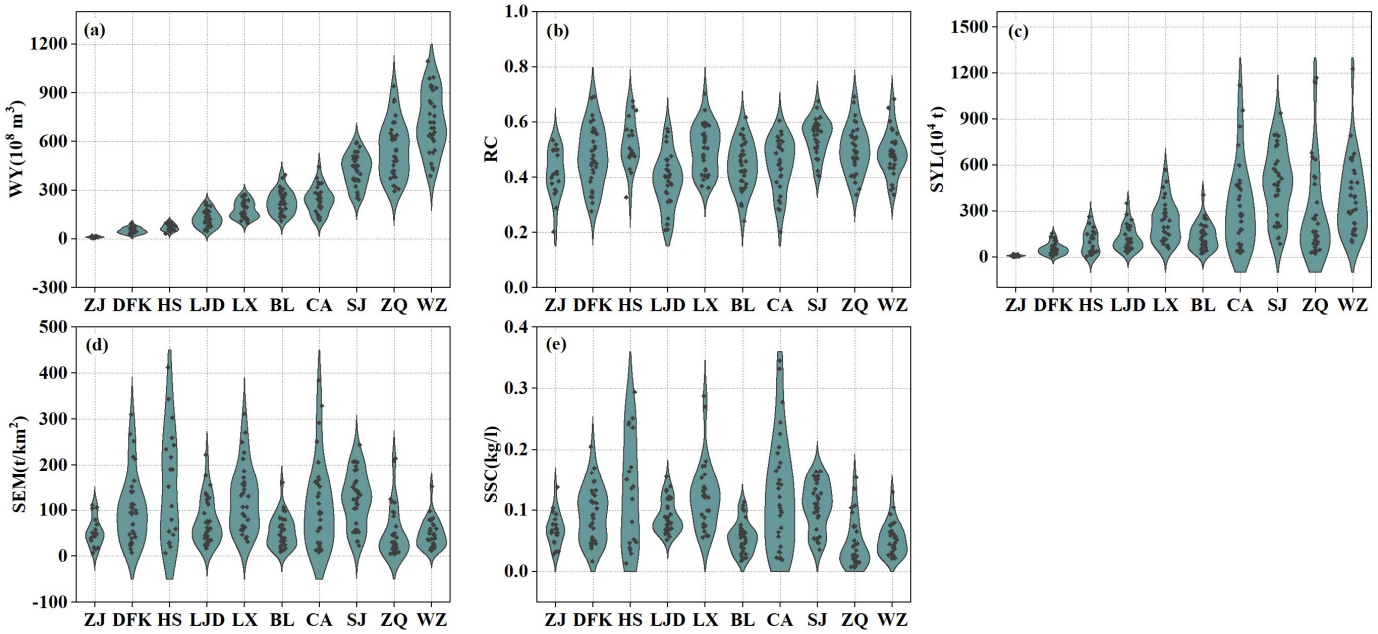

Figure 2. Variations in hydrological indices from 1990 to 2019. (**a**–**e**) represent WY, RC, SYL, SEM, and SSC, respectively.

The change trends of the hydrological indices are shown in Table 2, and their temporal variations are shown in Figure A1. WY showed a decreased trend in the DFK, BL, CA, SJ, and WZ watersheds while exhibiting an increased trend in the ZJ, HS, LJD, LX, and ZQ watersheds. RC increased in all watersheds except for CA and SJ. In particular, DFK, BL, and WZ suffered decreases in WY, whereas their RC values increased. As a whole, the change trends of WY and RC were not significant for all watersheds. Differing from WY and RC, SYL and SEM decreased in all watersheds except for the ZJ, HS, and LX watersheds. SYL and SEM values increased significantly ($p < 0.01$) in HS and decreased significantly ($p < 0.01$) in CA and WZ. Interestingly, LJD and ZQ increased in WY and RC but decreased in SYL and SEM. This phenomenon may have been caused by LP changes and human activity in these regions. As for SSC, it significantly increased in HS ($p < 0.01$) and

significantly ($p < 0.05$) decreased in LJD, ZQ, BL, CA, and WZ. In general, soil erosion was mitigated in most watersheds, whereas water resources decreased in the larger watersheds and increased in the smaller watersheds.

Table 2. Change trend statistics of hydrological indices from 1990 to 2019.

Indices	ZJ	DFK	HS	LJD	LX	BL	CA	SJ	ZQ	WZ
WY	0.25	−0.003	1.53	0.16	0.64	−0.12	−1.22	−1.00	0.75	−1.13
RC	0.0048	0.0012	0.0064	0.0008	0.0016	0.0013	−0.0009	−0.0001	0.0008	0.0004
SYL	0.04	−0.02	10.90 **	−1.19	4.43	−3.04	−19.01 **	−4.72	−7.63	−19.76 **
SEM	0.23	−0.04	17.03 **	−0.75	2.43	−1.20	−6.53 **	−1.23	−1.40	−2.44 **
SSC	−0.0005	0.0002	0.0128 **	−0.0011 *	0.0019	−0.0015 **	−0.0073 **	−0.0008	−0.0016 *	−0.0026 **

Note: The units of WY, SYL, SEM, and SSC are 10^8 m^3, 10^4 t, t/km^2, and mg/l, respectively, and RC is a dimensionless quantity. The change trends of these indices are shown as the average variations for each year. * and ** represent significant correlations at confidence levels of 95% and 99%, respectively.

4.2. Temporal Variations in LPs in the Chosen Watersheds

4.2.1. Land Use Changes from 1990 to 2019

As shown in Figure 3, the dominant land use type of the chosen watersheds was forest land, followed by agricultural land. The ratio of agricultural land was higher in ZJ, LJD, LX, BL, and WZ compared to the other watersheds, which were also more intensively distributed. In addition, from 1990 to 2019, urban land expanded drastically in all watersheds, especially in ZJ, LJD, LX, and WZ. The regions in which the land use types for different watersheds were altered occupied about 3.01–8.46% (average of 6.03%), 4.22–9.78% (average of 6.81%), and 5.11–11.47% (average of 8.83%) of the total area from 1990 to 2005, from 2005 to 2019, and from 1990 to 2019, respectively. Interestingly, the average area of the regions whose land use types had been altered from 1990 to 2019 was much lower than the sum of these regions from 1990 to 2005 and from 2005 to 2019. This may suggest that some unreasonable land use conversions from 1990 to 2005 had been corrected from 2005 to 2019. From 1990 to 2019, urban expansion was the only long-lasting land use conversion process.

Figure 4 shows the details of land use conversions among different land use types from 1990 to 2005 and from 2005 to 2019. We found that land use conversions mainly happened on agricultural land, forest land, and urban land. From 1990 to 2005, the main land use conversions were forest land–agricultural land, agricultural land–urban land, and agricultural land–forest land; part of the agricultural land had also been converted into water areas within ZJ, HS, LJD, LX, BL, and SJ. From 2005 to 2019, the main land use conversions were agricultural land–urban land, agricultural land–forest land, and forest land–agricultural land; some urban land was converted from forest land within DFK, HS, LX, CA, ZQ, and WZ. These results reveal that the urban expansion in southeastern China was mainly facilitated by occupying agricultural land, especially from 1990 to 2005. During recent decades, urban expansion also happened in some forest regions for most watersheds. This was reasonable, as urban development had extended to the surrounding rural areas first in most regions, which had large areas of agricultural land and forest land [65–67]. In addition, conversions between agricultural land and forest land were relatively greater. These results may have been caused by land use exchanges. For better soil erosion prevention, some sloped agricultural land was abandoned and converted into forest land, whereas some flat forest land was converted into agricultural land to preserve the amount of agricultural land and promote guaranteed crop production.

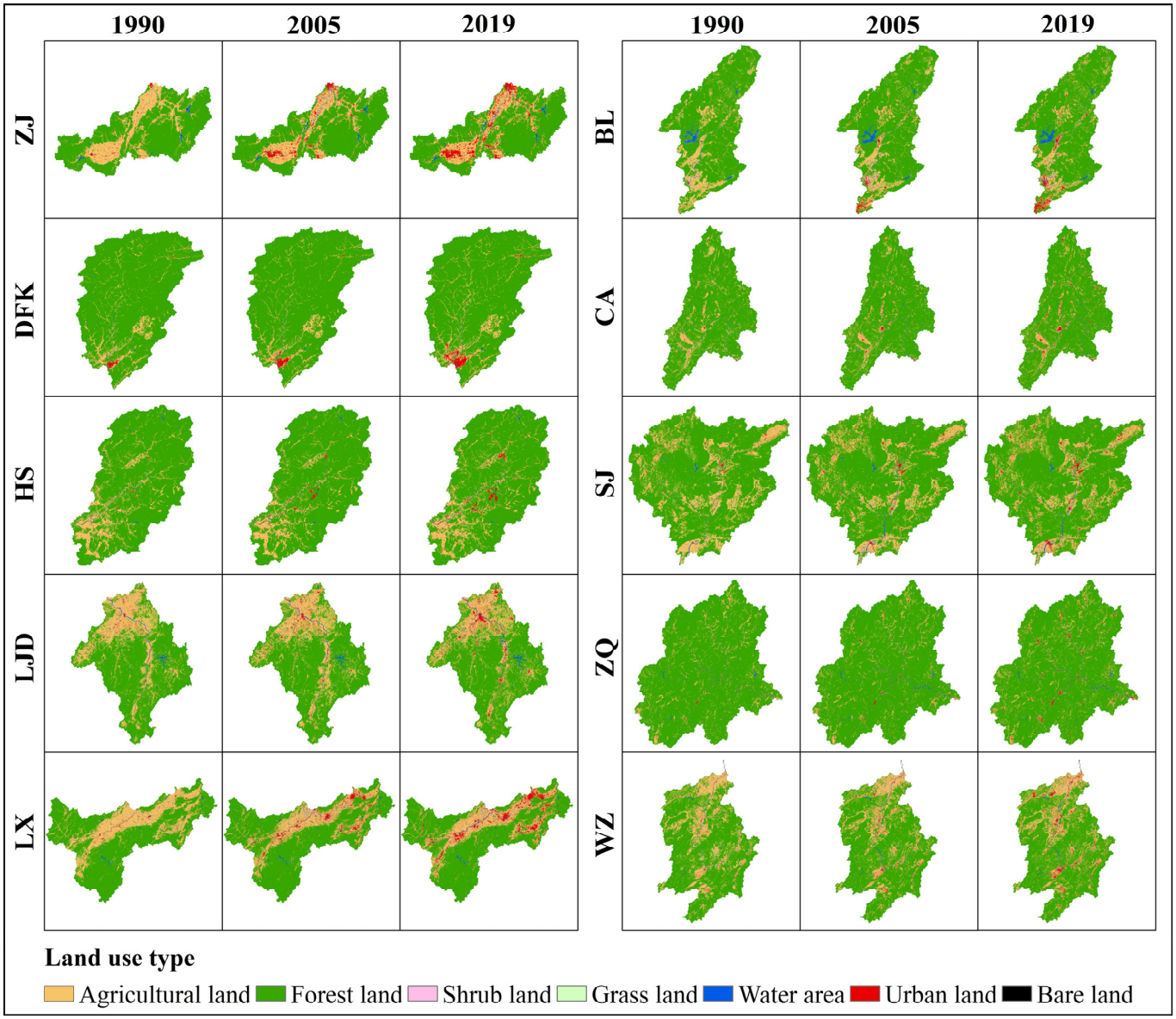

Figure 3. Land use maps of ZJ, DFK, HS, LJD, LX, BL, CA, SJ, ZQ, and WZ in 1990, 2005, and 2019.

4.2.2. LM Changes from 1990 to 2019

As shown in Figure 5, the variations in all LMs of ZJ were the largest among all watersheds. In addition, several LMs of LX, ZQ, and WZ also showed larger variations compared to the other watersheds. The average values of LPI and PAFRAC had similar trends with increases in watershed size. The analogical character was also shown for DIVISION, IJI, PD, SHDI, SHEI, and MSIEI. It is notable that the LPs within ZJ changed intensively in 1998, 2001, 2007, and 2017, with obvious variations in LPI, DIVISION, and COHESION. The LPs within LX changed intensively in 1993, 2007, and 2016 (Figure A2). Different from the other LMs, COHESION changed little in all watersheds except ZJ compared to the other LMs. This may suggest that COHESION was not as sensitive as other LMs to LPs changes.

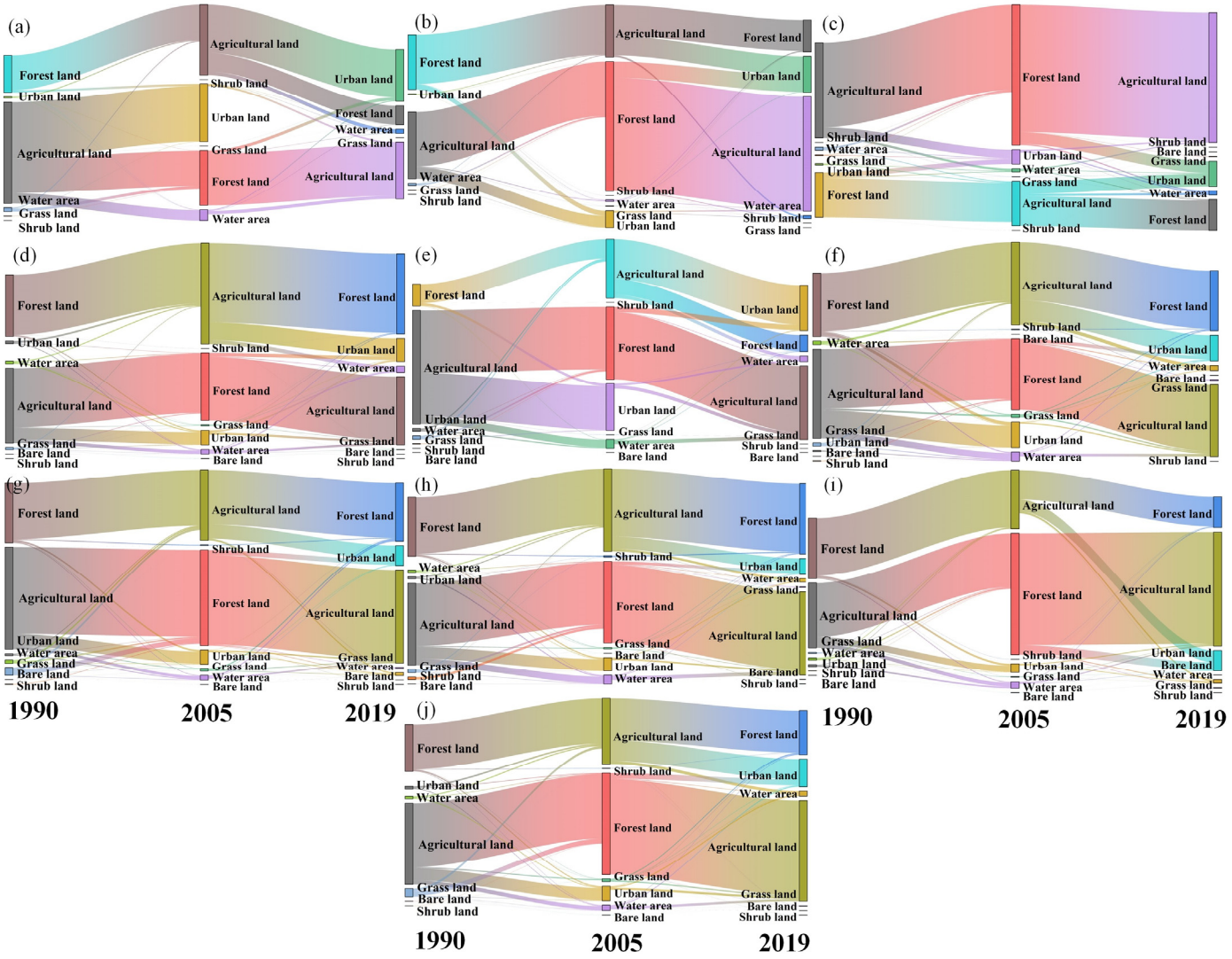

Figure 4. Land use conversion statistics between 1990, 2005, and 2019 for the chosen watersheds. Land whose land use type did not change is not included in this figure. (**a**–**j**) represent the ZJ, DFK, HS, LJD, LX, BO, CA, SJ, ZQ, and WZ watersheds, respectively.

The change trend statistic results of the chosen LMs from 1990 to 2019 are shown in Table 3. For most watersheds, most LMs changed significantly ($p < 0.05$), which demonstrates that LPs characteristics changed significantly during this period. Among all watersheds, the LPs within ZQ was the most intensively changed, as all LMs of ZQ changed significantly ($p < 0.01$). In detail, COHESION (ED, PAFRAC, AI, IJI, CONTAG, LSI, and SHEI) and SHDI (LPI and DIVISION) significantly ($p < 0.05$) changed in nine (individually, eight and seven, respectively) watersheds; NP and PD (MSIEI) significantly ($p < 0.01$) changed in six (four) watersheds. Among these significant trends, ED, DIVISION, IJI, LSI, SHDI, SHEI, and MSIEI (AI, CONTAG, COHESION, LPI, and PAFRAC) all significantly ($p < 0.05$) increased (or decreased) in most watersheds. These uniformities in the change trends of the LMs may suggest that the development directions in land use planning were similar across the regions of southeastern China. In addition, COHESION significantly decreased in most watersheds, which did not show obvious variations. The change trends of SHDI and SHEI were similar in all watersheds, and the change trend of SHDI was more obvious than that of SHEI (Figure A2). In general, the LPs within the chosen watersheds significantly changed from a landscape perspective.

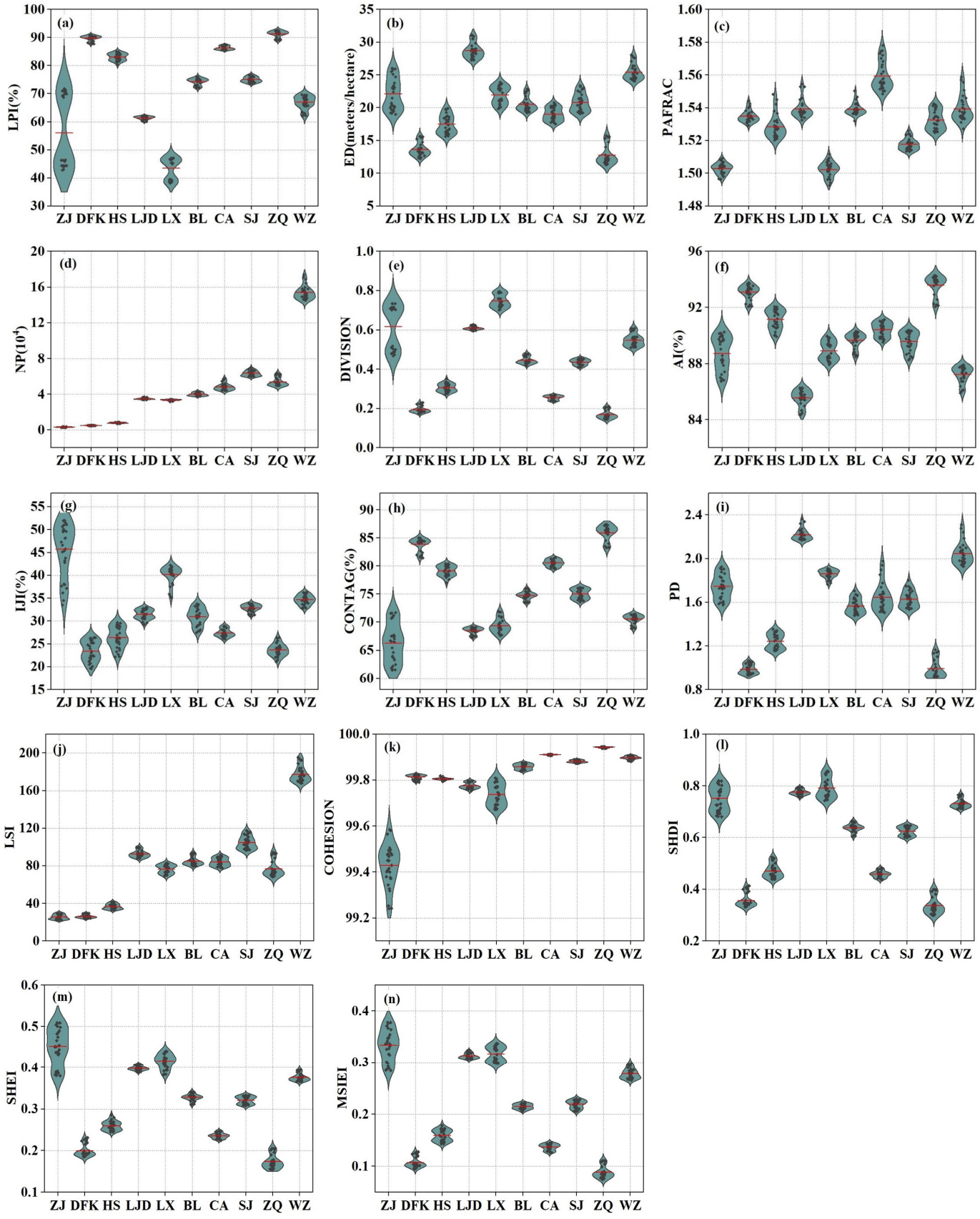

Figure 5. Variations of LMs from 1990 to 2019. (**a**–**n**) represent LPI, ED, PAFRAC, NP, DIVISION, AI, IJI, CONTAG, PD, LSI, COHESION, SHDI, SHEI, and MSIEI, respectively.

Table 3. Change trend statistics of LMs within the chosen watersheds from 1990 to 2019.

Metrics	ZJ	DFK	HS	LJD	LX	BL	CA	SJ	ZQ	WZ
LPI	0.62 *	−0.06 **	−0.01	−0.04 *	−0.09	−0.08 **	0.02	−0.07 **	−0.11 **	−0.11 *
ED	0.26 **	0.05 *	0.03	0.12 **	0.15 **	0.11 **	−0.01	0.14 **	0.13 **	0.06 *
PAFRAC	0.0001	0.0002 **	−0.0005 **	−0.0005 **	−0.0004 **	−0.0002 **	−0.0009 **	0.00005	−0.0004 **	−0.0008 **
NP	0.0013 **	0.0004	−0.0006	−0.0045 **	0.0045 **	0.0072	−0.0264 **	0.0108	0.0263 **	−0.0436 **
DIVISION	−0.0043	0.0010 **	0.0002	0.0007 **	0.0021 **	0.0013 **	−0.0003	0.0011 **	0.020 **	0.0014 *
AI	−0.129 **	−0.025 *	−0.015	−0.058 **	−0.074 **	−0.054 **	0.007	−0.068 **	−0.065 **	−0.029 *
IJI	0.55 **	0.24 **	0.18 **	0.11 **	0.08 *	0.16 **	0.05 *	−0.03	0.12 **	−0.02
CONTAG	−0.376 **	−0.082 **	−0.14	−0.063 **	−0.097 **	−0.073 **	−0.001	−0.087 **	−0.137 **	−0.049 **
PD	0.008 **	0.001	−0.001	−0.003 **	0.002 **	0.003	−0.009 **	0.003	0.005 **	−0.006 **
LSI	0.27 **	0.09 *	0.06	0.36 **	0.50 **	0.44 **	−0.06	0.67 **	0.76 **	0.39 *
COHESION	−0.0034	−0.0011 **	−0.0003 **	−0.0013 **	−0.0045 **	−0.0013 **	−0.0001 **	−0.0005 **	−0.0003 **	−0.0005 **
SHDI	0.005 **	0.002 **	0.001 *	0.001 **	0.004 **	0.002 **	0.001	0.002 **	0.003 **	0.001 **
SHEI	0.005 **	0.001 **	0.001	0.001 **	0.001 **	0.001 **	0.001	0.001 **	0.002 **	0.001 **
MSIEI	0.0031 **	0.0006 **	0	−0.0001	0.0005	0	−0.0001	0.0006 **	0.0011 **	0.0003

Note: The units of LPI, ED, DIVISION, AI, IJI, CONTAG, and PD are %, meters/hectare, proportion, %, %, %, and number/100 hectares, respectively, and PAFRAC, NP, LSI, COHESION, SHDI, SHEI, and MSIEI are dimensionless quantities. The change trends of these indicators are shown as the average variations each year. * and ** represent significant correlations at confidence levels of 95% and 99%, respectively.

4.3. Relationships between Hydrological Indices and LPs

The CC between the hydrological indices (WY, RC, SEM, and SSC) and LMs (LPI, ED, PAFRAC, NP, DIVISION, AI, IJI, CONTAG, PD, LSI, COHESION, SHDI, SHEI, and MSIEI) of the chosen watersheds are shown in Tables 4 and 5. There were discrepancies in the lag times of the correlations between the hydrological indices and LMs in different watersheds in the subtropical monsoon climate zone of southeastern China. In addition, the lag times between the hydrological indices and LMs did not show an obvious relationship with watershed size.

Table 4. CC values between the landscape metrics and the WY and RC.

Hydrological Indices	LMs	ZJ	DFK	HS	LJD	LX	BL	CA	SJ	ZQ	WZ
WY	LPI	**0.57** ^{1}	−0.28 ^{0}	−0.46 ^{0}	−0.29 ^{1}	**−0.46** ^{3}	−0.22 ^{1}	−0.21 ^{0}	0.28 ^{1}	−0.08 ^{0}	**−0.40** ^{4}
	ED	0.48 ^{1}	0.27 ^{0}	0.39 ^{0}	−0.03 ^{1}	0.14 ^{4}	0.13 ^{0}	0.25 ^{2}	−0.13 ^{1}	0.10 ^{0}	0.29 ^{2}
	PAFRAC	−0.12 ^{2}	0.12 ^{0}	**0.50** ^{0}	0.16 ^{3}	−0.33 ^{1}	0.21 ^{2}	0.24 ^{2}	0.34 ^{4}	0.19 ^{2}	0.26 ^{2}
	NP	**0.53** ^{1}	0.33 ^{1}	0.33 ^{0}	0.16 ^{2}	0.37 ^{4}	0.20 ^{3}	0.27 ^{2}	0.30 ^{4}	0.19 ^{2}	0.35 ^{2}
	DIVISION	**−0.56** ^{1}	0.28 ^{0}	0.46 ^{0}	0.16 ^{1}	0.36 ^{3}	0.22 ^{1}	0.21 ^{0}	−0.28 ^{1}	0.08 ^{0}	**0.39** ^{4}
	AI	−0.48 ^{1}	−0.27 ^{0}	−0.39 ^{0}	0.03 ^{1}	−0.14 ^{4}	−0.13 ^{0}	−0.25 ^{2}	0.13 ^{1}	−0.10 ^{0}	−0.29 ^{2}
	IJI	0.47 ^{1}	−0.11 ^{0}	**0.60** ^{4}	0.08 ^{4}	0.11 ^{0}	−0.17 ^{2}	−0.26 ^{0}	−0.26 ^{3}	0.14 ^{4}	−0.35 ^{0}
	CONTAG	−0.47 ^{1}	−0.23 ^{0}	**−0.53** ^{1}	−0.12 ^{0}	−0.24 ^{0}	−0.12 ^{0}	−0.22 ^{2}	0.18 ^{1}	−0.09 ^{0}	−0.31 ^{4}
	PD	**0.53** ^{1}	0.33 ^{1}	0.33 ^{0}	0.16 ^{2}	0.37 ^{4}	0.20 ^{3}	0.27 ^{2}	0.30 ^{4}	0.19 ^{2}	0.35 ^{2}
	LSI	0.48 ^{1}	0.27 ^{0}	0.39 ^{0}	−0.03 ^{1}	0.14 ^{4}	0.13 ^{0}	0.25 ^{2}	−0.13 ^{1}	0.10 ^{0}	0.29 ^{2}
	COHESION	**0.59** ^{3}	−0.16 ^{4}	**−0.51** ^{0}	0.16 ^{2}	−0.21 ^{4}	−0.08 ^{4}	−0.09 ^{4}	0.30 ^{2}	−0.11 ^{3}	−0.33 ^{4}
	SHDI	**0.50** ^{1}	0.20 ^{0}	0.41 ^{0}	0.26 ^{1}	0.17 ^{4}	−0.16 ^{3}	0.18 ^{0}	−0.21 ^{1}	0.08 ^{0}	0.32 ^{4}
	SHEI	0.46 ^{1}	0.20 ^{0}	**0.54** ^{1}	0.26 ^{1}	0.27 ^{0}	−0.16 ^{3}	0.18 ^{0}	−0.21 ^{1}	0.08 ^{0}	0.32 ^{4}
	MSIEI	0.34 ^{0}	0.25 ^{0}	**0.48** ^{0}	0.32 ^{1}	0.34 ^{0}	−0.13 ^{3}	0.21 ^{0}	−0.23 ^{1}	0.08 ^{1}	0.30 ^{2}
RC	LPI	**0.58** ^{1}	**−0.44** ^{0}	**−0.55** ^{0}	−0.28 ^{0}	**−0.52** ^{3}	−0.34 ^{1}	−0.27 ^{2}	0.19 ^{1}	−0.18 ^{0}	**−0.41** ^{1}
	ED	0.45 ^{1}	**0.43** ^{0}	**0.50** ^{0}	0.11 ^{3}	0.18 ^{4}	0.30 ^{0}	0.30 ^{2}	0.13 ^{4}	0.19 ^{0}	**0.39** ^{2}
	PAFRAC	−0.17 ^{3}	0.28 ^{0}	**0.53** ^{1}	−0.12 ^{0}	−0.33 ^{0}	0.14 ^{2}	0.21 ^{2}	0.37 ^{4}	0.14 ^{2}	0.16 ^{2}
	NP	**0.49** ^{1}	**0.44** ^{1}	0.48 ^{2}	0.17 ^{2}	0.33 ^{4}	0.27 ^{3}	0.25 ^{2}	0.31 ^{4}	0.25 ^{2}	0.31 ^{2}
	DIVISION	**−0.57** ^{1}	**0.44** ^{0}	**0.55** ^{0}	0.22 ^{0}	**0.41** ^{3}	0.34 ^{1}	0.27 ^{2}	−0.19 ^{1}	0.18 ^{0}	**0.41** ^{1}
	AI	−0.45 ^{1}	**−0.43** ^{0}	**−0.50** ^{0}	−0.11 ^{3}	−0.18 ^{4}	−0.30 ^{0}	−0.30 ^{2}	−0.13 ^{4}	−0.19 ^{0}	**−0.39** ^{2}
	IJI	0.48 ^{1}	0.18 ^{4}	**0.63** ^{4}	0.13 ^{4}	−0.19 ^{3}	−0.09 ^{2}	−0.28 ^{0}	−0.25 ^{3}	0.18 ^{4}	**−0.42** ^{0}
	CONTAG	−0.46 ^{1}	**−0.40** ^{0}	**−0.57** ^{1}	−0.19 ^{0}	−0.22 ^{0}	−0.28 ^{0}	−0.29 ^{2}	0.09 ^{1}	−0.18 ^{0}	**−0.40** ^{3}
	PD	**0.49** ^{1}	**0.44** ^{1}	0.48 ^{2}	0.18 ^{2}	0.33 ^{4}	0.27 ^{3}	0.25 ^{2}	0.31 ^{4}	0.25 ^{2}	0.31 ^{2}
	LSI	0.45 ^{1}	**0.43** ^{0}	**0.50** ^{0}	0.11 ^{3}	0.18 ^{4}	0.30 ^{0}	0.30 ^{2}	0.13 ^{4}	0.19 ^{0}	**0.39** ^{2}
	COHESION	**0.59** ^{3}	−0.34 ^{4}	**−0.54** ^{0}	0.12 ^{1}	−0.24 ^{4}	−0.19 ^{1}	−0.17 ^{4}	0.22^{2}	−0.18 ^{3}	−0.37 ^{4}
	SHDI	0.47 ^{1}	**0.38** ^{0}	**0.51** ^{0}	0.28 ^{0}	0.24 ^{4}	0.25 ^{0}	0.28 ^{2}	−0.11 ^{1}	0.18 ^{0}	**0.40** ^{3}
	SHEI	0.45 ^{1}	**0.38** ^{0}	**0.58** ^{1}	0.28 ^{0}	0.27 ^{0}	0.24 ^{0}	0.28 ^{2}	−0.11 ^{1}	0.18 ^{0}	**0.40** ^{3}
	MSIEI	0.33 ^{1}	**0.42** ^{0}	**0.56** ^{1}	0.28 ^{0}	0.35 ^{0}	0.18 ^{0}	0.27 ^{2}	−0.13 ^{1}	0.18 ^{1}	**0.39** ^{2}

Note: bold font indicates a correlation was significant at a confidence level of 95%, bold and underlined font indicates a correlation was significant at a confidence level of 99%, and a superscript number indicates the lag time of the correlation between the LMs and the WY or RC.

Table 5. CC values between LMs and the SEM and SSC.

Hydrological Indices	LMs	ZJ	DFK	HS	LJD	LX	BL	CA	SJ	ZQ	WZ
SEM	LPI	**0.62** ^{1}	−0.30 ^{2}	**−0.72** ^{0}	−0.18 ^{1}	**−0.63** ^{3}	0.16 ^{0}	**−0.44** ^{3}	−0.35 ^{3}	0.13 ^{0}	−0.21 ^{4}
	ED	0.24 ^{1}	0.27 ^{3}	**0.69** ^{0}	−0.15 ^{0}	0.34 ^{4}	−0.25 ^{0}	**0.42** ^{2}	−0.17 ^{0}	−0.12 ^{0}	0.35 ^{4}
	PAFRAC	−0.33 ^{0}	−0.10 ^{2}	**0.76** ^{0}	0.29 ^{2}	**−0.46** ^{0}	0.30 ^{2}	**0.63** ^{0}	0.34 ^{3}	0.17 ^{2}	**0.82** ^{2}
	NP	0.30 ^{1}	**0.41** ^{3}	**0.66** ^{0}	0.27 ^{2}	**0.59** ^{4}	−0.16 ^{0}	**0.58** ^{0}	0.32 ^{3}	0.13 ^{2}	**0.71** ^{2}
	DIVISION	**−0.63** ^{1}	0.30 ^{2}	**0.72** ^{0}	−0.13 ^{2}	**0.59** ^{3}	−0.17 ^{0}	**0.44** ^{3}	0.34 ^{3}	−0.13 ^{0}	0.20 ^{4}
	AI	−0.24 ^{1}	−0.27 ^{3}	**−0.69** ^{0}	0.15 ^{0}	**−0.34** ^{4}	0.25 ^{0}	**−0.42** ^{2}	0.17 ^{0}	0.12 ^{0}	−0.35 ^{4}
	IJI	**−0.75** ^{4}	−0.16 ^{3}	**0.76** ^{4}	−0.16 ^{2}	0.33 ^{0}	−0.36 ^{2}	**−0.45** ^{2}	0.12 ^{1}	−0.29 ^{2}	−0.30 ^{4}
	CONTAG	**0.64** ^{4}	−0.23 ^{2}	**−0.76** ^{0}	0.07 ^{2}	**−0.44** ^{0}	0.30 ^{2}	−0.38 ^{3}	0.18 ^{0}	0.14 ^{0}	0.21 ^{0}
	PD	0.30 ^{1}	**0.41** ^{3}	**0.66** ^{0}	0.27 ^{2}	**0.59** ^{4}	−0.16 ^{0}	**0.58** ^{0}	0.32 ^{3}	0.13 ^{2}	**0.71** ^{2}
	LSI	0.24 ^{1}	0.27 ^{3}	**0.69** ^{0}	−0.15 ^{0}	0.34 ^{4}	−0.25 ^{0}	**0.42** ^{2}	−0.17 ^{0}	−0.12 ^{0}	0.35 ^{4}
	COHESION	**0.53** ^{1}	−0.09 ^{1}	**−0.73** ^{0}	0.28 ^{2}	**−0.48** ^{4}	0.33 ^{2}	**0.47** ^{0}	0.21 ^{2}	0.14 ^{0}	0.35 ^{2}
	SHDI	0.27 ^{1}	0.20 ^{2}	**0.72** ^{0}	0.14 ^{1}	**0.36** ^{0}	−0.31 ^{2}	0.31 ^{3}	−0.18 ^{0}	−0.14 ^{0}	−0.24 ^{0}
	SHEI	**−0.69** ^{4}	0.20 ^{2}	**0.77** ^{0}	0.14 ^{1}	**0.47** ^{0}	−0.31 ^{2}	0.31 ^{3}	−0.18 ^{0}	−0.14 ^{0}	−0.24 ^{0}
	MSIEI	**−0.74** ^{4}	0.26 ^{2}	**0.75** ^{0}	0.35 ^{1}	**0.42** ^{0}	0.15 ^{4}	**0.41** ^{3}	0.25 ^{3}	−0.25 ^{0}	0.25 ^{4}
SSC	LPI	**0.52** ^{1}	−0.34 ^{2}	**−0.65** ^{0}	0.18 ^{2}	**−0.58** ^{2}	0.30 ^{0}	**−0.50** ^{3}	**−0.45** ^{3}	0.21 ^{0}	0.23 ^{0}
	ED	−0.37 ^{4}	0.34 ^{3}	**0.68** ^{0}	−0.35 ^{0}	0.34 ^{4}	**−0.44** ^{0}	**0.48** ^{4}	−0.15 ^{0}	−0.17 ^{0}	0.26 ^{4}
	PAFRAC	**−0.49** ^{0}	0.16 ^{0}	**0.78** ^{0}	**0.54** ^{2}	**−0.41** ^{0}	0.35 ^{2}	**0.70** ^{0}	0.27 ^{3}	0.26 ^{0}	**0.89** ^{2}
	NP	−0.41 ^{4}	**0.45** ^{3}	**0.66** ^{0}	**0.51** ^{4}	**0.61** ^{3}	−0.22 ^{0}	**0.62** ^{0}	0.26 ^{3}	0.12 ^{2}	**0.74** ^{4}
	DIVISION	**−0.53** ^{1}	0.34 ^{2}	**0.65** ^{0}	−0.34 ^{2}	**0.55** ^{2}	−0.32 ^{0}	**0.50** ^{3}	**0.44** ^{3}	−0.21 ^{0}	−0.23 ^{0}
	AI	0.37 ^{4}	−0.34 ^{3}	**−0.68** ^{0}	0.35 ^{0}	−0.34 ^{4}	**0.44** ^{0}	**−0.48** ^{4}	0.15 ^{0}	0.17 ^{0}	−0.27 ^{4}
	IJI	**−0.71** ^{4}	−0.09 ^{3}	**0.73** ^{4}	−0.36 ^{2}	**0.39** ^{0}	**−0.49** ^{2}	**−0.51** ^{2}	0.19 ^{1}	**−0.38** ^{2}	−0.36 ^{4}
	CONTAG	**0.73** ^{4}	−0.30 ^{3}	**−0.70** ^{0}	0.24 ^{2}	**−0.46** ^{0}	**0.46** ^{0}	**−0.45** ^{4}	−0.16 ^{4}	0.22 ^{0}	0.33 ^{0}
	PD	−0.41 ^{4}	**0.45** ^{3}	**0.66** ^{0}	**0.51** ^{4}	**0.61** ^{3}	−0.22 ^{0}	**0.62** ^{0}	0.26 ^{3}	0.12 ^{2}	**0.74** ^{4}
	LSI	−0.37 ^{4}	0.34 ^{3}	**0.68** ^{0}	−0.35 ^{0}	0.34 ^{4}	**−0.44** ^{0}	**0.48** ^{4}	−0.15 ^{0}	−0.17 ^{0}	0.26 ^{4}
	COHESION	**0.53** ^{0}	−0.20 ^{1}	**−0.66** ^{0}	**0.46** ^{0}	**−0.47** ^{4}	**0.49** ^{0}	**0.59** ^{0}	0.15 ^{0}	0.26 ^{0}	**0.49** ^{2}
	SHDI	−0.36 ^{4}	0.28 ^{3}	**0.72** ^{0}	−0.20 ^{4}	**0.37** ^{0}	**−0.44** ^{0}	0.38 ^{4}	0.19 ^{4}	−0.23 ^{0}	**−0.37** ^{0}
	SHEI	**−0.75** ^{4}	0.28 ^{3}	**0.70** ^{0}	−0.20 ^{4}	**0.47** ^{0}	**−0.44** ^{0}	0.38 ^{4}	0.19 ^{4}	−0.23 ^{0}	**−0.37** ^{0}
	MSIEI	**−0.74** ^{4}	0.32 ^{3}	**0.70** ^{0}	**0.43** ^{0}	**0.38** ^{0}	0.32 ^{4}	**0.47** ^{3}	0.33 ^{3}	−0.35 ^{0}	−0.15 ^{0}

Note: bold font indicates a correlation was significant at a confidence level of 95%, bold and underlined font indicates a correlation was significant at a confidence level of 99%, and a superscript number indicates the lag time of the correlation between the LMs and the WY or RC.

In most watersheds, WY and RC were negatively correlated with LPI, AI, and COHESION and positively correlated with ED, PAFRAC, NP, DIVISION, PD, LSI, SHDI, SHEI, and MSIEI; SEM was negatively correlated with LPI and IJI and positively correlated with PAFRAC, NP, PD, COHESION, and MSIEI; SSC was negatively correlated with IJI and positively correlated with PAFRAC, NP, PD, COHESION, and MSIEI. In addition, the correlation between WY/RC and IJI varied in watersheds with different sizes. In general, runoff decreases when a landscape becomes more fragmented or its shape gains complexity [51], and sediment transportation is disturbed when a landscape patch becomes larger or fragmented, further reducing sediment yields [35]. In addition, the results show that the effect of LPs on SSC and SEM were similar, which indicates that the LPs affect SSC by affecting SEM. It can be seen in Table 4 that most watersheds with larger areas had negative correlations between WY/RC and IJI, whereas most watersheds with smaller areas had positive correlations between WY/RC and IJI. A similar phenomenon was found between SHDI/SHEI and SEM. Most watersheds with larger areas had negative correlations between SHDI/SHEI and SEM, whereas most watersheds with smaller areas had positive correlations between SHDI/SHEI and SEM.

The effects of LMs on different hydrological indices varied, even in the same watersheds. For instance, for DKF, no significant ($p < 0.05$) correlations were found between WY and any LMs, but all LMs except for PAFRAC, IJI, and COHESION were significantly ($p < 0.05$) correlated with RC; for WZ, all LMs except for LPI and DIVISION did not show significant ($p < 0.05$) correlations with WY, whereas all LMs except for PAFRAC, NP, PD, and COHESION were significantly ($p < 0.05$) correlated with RC. In general, the effects of the LMs on SEM and SSC were more significant than their effects on WY and RC. Among the chosen watersheds, only four watersheds (LJD, BL, SJ, and ZQ) did not show significant ($p < 0.05$) correlations between SEM and the LMs. In particular, all LMs were significantly ($p < 0.01$) correlated with the SEM in HS; seven, ten, and eleven LMs were significantly ($p < 0.05$) correlated

with the SEMs in ZJ, LX, and CA, respectively. Based on the CC between SSC and all LMs, it seems that LPs changes could closely affect the relationship between streamflow and sediment yields. SSC was found to be significantly ($p < 0.05$) correlated with at least one LM in all of the chosen watersheds. In particular, all LMs were significantly ($p < 0.01$) correlated with the SSC in HS, and eight, eleven, eight, and twelve LMs were significantly ($p < 0.05$) correlated with the SSCs in ZJ, LX, BL, and CA, respectively.

5. Discussion

5.1. Correlations between LMs and Watershed Size

Different LMs represent different LPs characteristics, which may be different in different regions due to the varied landscape. In our study, the average LMs were correlated with watershed size (Figure 6). In detail, ED, DIVISION, PD, SHDI, SHEI, and MSIEI had similar correlations to watershed size. These LMs were negatively correlated with watershed size when it ranged from 20,000 to 60,000 km^2 and positively correlated with watershed size when it was in other ranges. LPI, AI, and CONTAG had similar correlations with watershed size. These LMs showed reverse correlations with watershed size compared to ED, DIVISION, PD, SHDI, SHEI, and MSIEI. Generally, ED, DIVISION, PD, SHDI, SHEI, and MSIEI represent the fragmentation of the landscape, whereas LPI, AI, and CONTAG represent the aggregation of the landscape. This result indicates that the LMs that represent similar landscape characteristics had similar correlations with watershed size, whereas the LMs with opposite landscape characteristics had reverse correlations with watershed size. The thresholds of 20,000 and 60,000 km^2 may suggest that fragmentation of the landscape would be decreased in southeastern China where the area ranges from 20,000 to 60,000 km^2. PAFRAC and COHESION showed similar correlations with watersheds, with slow increasing trends where the watershed size ranged from 0 to 30,000 km^2. Interestingly, NP and LSI were significantly ($p < 0.01$) positively correlated with watershed size. The increasing trend was smaller where the watershed size ranged from 25,000 to 55,000 km^2 compared to other ranges. NP represents the number of patches in the watershed, and LSI represents the ratio of edge and area of landscape. Generally, NP and LSI would increase with the increase in watershed size, but the slight increasing trend of NP and LSI where the watershed size ranges from 25,000 to 55,000 km^2 may suggest that the number of patches and the ratio of the edge to the area of a landscape would not be changed obviously where the area of watershed ranges from 25,000 to 55,000 km^2. When the watershed area fell in this scope, the increased area mainly had less fragmentation. These correlations between LMs and watershed size may suggest that the effects of LMs on hydrological processes also have scale effects, as suggested by Xiao, Cao, Liu, and Lu [34]. More LMs should be taken into consideration within more watersheds with wider size ranges to further verify this interesting hypothesis.

5.2. Effects of Various LMs on Hydrological Processes

The relationships between four hydrological indices (WY, RC, SEM, and SSC) and fourteen LMs (LPI, ED, PAFRAC, NP, DIVISION, AI, IJI, CONTAG, PD, LSI, COHESION, SHDI, SHEI, and MSIEI) within ten representative watersheds with various area sizes in the subtropical monsoon climate zone of southeastern China were evaluated using the slip correlation analysis method. In our study, for most watersheds, the land use maps and hydrological series for 30 consecutive years were used to investigate the relationships between landscapes and hydrological processes. Compared to previous studies, the amount of land use maps was much greater, and the hydrological series were measured rather than simulated with various models, which could greatly reduce the uncertainty brought by various models. In addition, the measured hydrological series under different landscapes could directly reflect the effect of landscape on hydrological processes. Taking the SWAT model as an example, as mentioned in the Introduction section, it simulates hydrological processes based on different combinations of land use, soil types, and slope belt. The SWAT model considers the land use amount but ignores the effects of land use spatial variations

on hydrological processes. For example, an HRU in a subwatershed would distribute in several places within the subwatershed, which makes it hard to represent the effect of land use spatial distributions on hydrological processes. Hence, it is more reliable to investigate the relationships between landscapes and hydrological processes using measured data compared to using simulated data from various models.

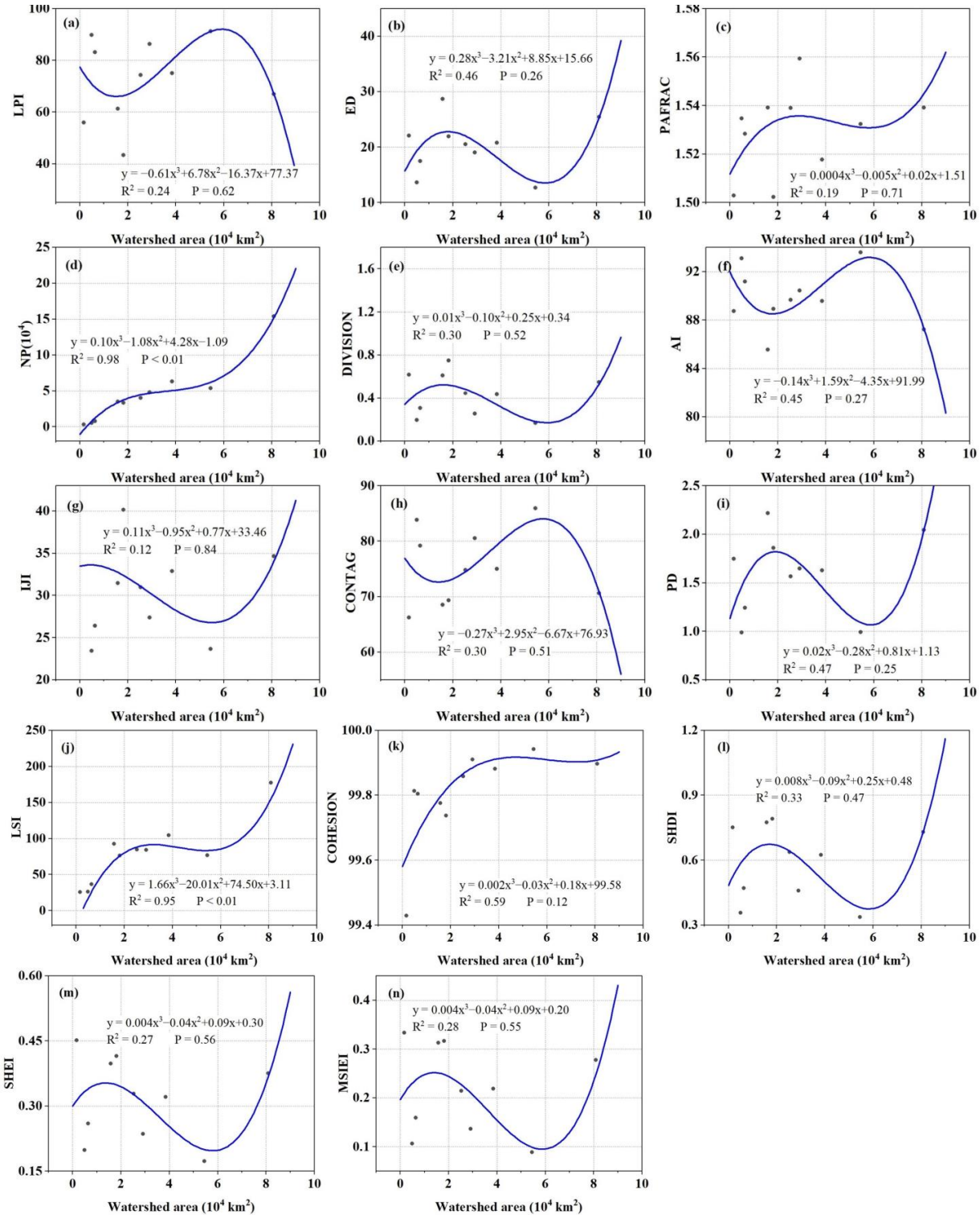

Figure 6. Statistics of the watershed area and average LMs for the chosen watersheds from 1990 to 2019. (**a**–**n**) represent LPI, ED, PAFRAC, NP, DIVISION, AI, IJI, CONTAG, PD, LSI, COHESION, SHDI, SHEI, and MSIEI, respectively.

Similar to previous studies, the relationships between the different hydrological indices and LMs in various watersheds had discrepancies [35]. In our study, some hydrological indices and LMs had the same correlations in most watersheds, and a few hydrological indices and some LMs even had the same correlation in all watersheds. For most watersheds ($\geq$7), WY was negatively correlated with LPI, AI, CONTAG, and COHESION and positively correlated with ED, PAFRAC, DIVISION, LSI, SHDI, SHEI, and MSIEI; RC was negatively correlated with LPI, CONTAG, and COHESION and positively correlated with PAFRAC, DIVISION, SHDI, SHEI, and MSIEI; SEM was negatively correlated with LPI and IJI; and SEM and SSC were positively correlated with PAFRAC, NP, PD, COHESION, and MSIEI. Interestingly, several LMs had the same relationships with WY and RC in all watersheds. As for SEM and SSC, there were no consistent correlations with any LMs for any watersheds. This discrepancy may have been caused by the soil erosion process being easier to disturb with human activity than the runoff process [68,69]. Hence, the relationships between LMs and SEM/SSC have discrepancies in various watersheds with differences in human activity intensity and mode.

LPI and ED were both related to the edge-area characteristic of LPs, and they had reverse effects on the runoff process. As mentioned before, LPI was negatively correlated with WY and RC, whereas ED was reversed. This result suggests that runoff increases in the subtropical monsoon climate zone when a watershed is dominated by a small patch of landscape. Similar results have also been reported in other regions [17], and a reverse result was also obtained [38]. In addition, SEM was negatively correlated with LPI in most watersheds, whereas it had no consistent correlation with ED. The dominant land use was forest and agricultural land, which may suggest that the dispersal of forest and agricultural land would increase soil erosion. The negative correlation between IJI and SEM also proved this result. A similar result was obtained by Zhang, Fan, Li and Yi [25]. In our study, seven aggregation LMs were chosen to analyze their correlation with four hydrological indices. For most watersheds, NP, PD, LSI, and DIVISION were positively correlated with WY and RC, whereas NP, PD, and COHESION were positively correlated with SEM and SSC. These results suggest that a proper increase in the fragmentation and physical connectivity of LPs was beneficial for water and soil conservation. A similar result was reported within the Upper Du River Basin in the middle of the Yangtze River [51], which is also within the subtropical monsoon climate zone. In addition, reverse results have been found in northern China, which belongs to the semi-arid continental monsoon climate zone [36,39] and may be caused by differences in rainfall patterns in different climate zones. The average annual precipitation in the study regions ranges from 1686 to 2162 mm (Table 1), whereas the average annual precipitation within the semi-arid continental monsoon climate zone ranges from 300 to 500 mm [70]. Furthermore, Ouyang, Skidmore, Hao, and Wang [33] pointed out that properly improving the fragile landscape status could prevent soil erosion, which may suggest that there is a threshold for landscape fragility. The changes in the fragmentation in the upper or lower fragmentation thresholds may be different, which may be another reason for the different correlations between relevant LMs and soil erosion. WY and RC were positively correlated with SHDI, SHEI, and MSIEI in most watersheds, which suggests that an increase in landscape diversity would increase runoff generation in the subtropical monsoon climate zone. As for SEM and SSC, the effect of landscape diversity varied in different regions [36,39,71], which may have resulted from discrepancies in land use type conversions. The main land use conversions from 1990 to 2019 within these watersheds were forest land–agricultural land, agricultural land–urban land, and agricultural land–forest land (Figure 4). Generally, small agricultural patches increased in a large forest patch, small urban patches increased in a large agricultural patch, and small forest patches increased in a large agricultural patch, which increased landscape diversity but may have affected soil erosion differently. A further investigation should be conducted to verify this hypothesis.

The correlations between LMs and RC were more obvious than those between LMs and WY (Table 4). There are no glaciers in the subtropical monsoon climate zone, and the main source of water yields was precipitation recharge [72]. Precipitation variation plays a more important role in interannual WY changes compared to LPs variations [73]. RC removed the effect of precipitation variations and watershed size to some extent compared to WY, and it was mainly affected by LULC, soil property, and slope [74]. These results suggest that relevant studies should choose RC to represent runoff generation character rather than WY. In addition, the relationships between LMs and SEM/SSC were not consistent in different watersheds. This may have been caused by the erosion process, which was also influenced by precipitation patterns, soil properties, slope, and topography [73,75–77]. WY/RC and SEM/SSC were both positively correlated with PAFRAC, NP, PD, and MSIEI in most watersheds. This shows that the soil erosion in these regions is mainly caused by rainfall erosion and surface runoff transportation [78]. In addition, the extensive construction projects brought about by rapid urban expansion also could have led to a lot of soil erosion [79], further influencing these results.

5.3. Recommendations for LM Selection in Future Relevant Studies

Our study selected 10 watersheds located in the subtropical monsoon climate zone in southeastern China. For the 10 chosen watersheds, the temporal variations and change trends of the 14 chosen LMs from 1990 to 2019 are shown in Figure A2 and Table 3. The results showed that the change trends of LPI and ED were opposite in all watersheds except for ZJ; the change trend of AI was opposite to LSI in all watersheds and similar to CONTAG and COHESION in all watersheds except for CA; and finally, SHDI and SHEI had similar change trends in all watersheds. In addition, the temporal variation in CONTAG was more obvious than those of AI and COHESION, but the change trend of COHESION was more significant compared to those of AI and CONTAG. SHDI was less disturbed by landscape changes compared to SHEI, as SHEI changed abruptly in some years, whereas similar changes did not appear for SHDI (Figure A2). In addition, the correlations with WY/RC for LPI and ED were opposite; the correlations with WY/RC for AI, CONTAG, and COHESION were similar, and COHESION had a positive correlation with SEM/SSC in most watersheds; the correlations with WY/RC for SHDI and SHEI were similar. Similar results were also reported in previous studies [17,35,37,80]. Hence, when analyzing the correlations between LPs and hydrological processes, it would be better to choose LPI, ED, PAFRAC, AI, COHESION, and SHDI as the representative LMs for fundamental LPs characteristics that include the edge area, shape, aggregation, and diversity aspects.

5.4. Implications, Limitations, and Prospects

Understanding the relationships between LPs and hydrological processes has a benefit for water and environmental management [27]. The results suggest that a proper decrease in landscape fragmentation and connectivity in the subtropical monsoon climate zone of southeastern China would benefit soil erosion prevention. In addition, meaningless land use conversions (forest land–agricultural land and agricultural land–forest land) should be decreased during local economic development, which would benefit decreasing landscape fragmentation and connectivity. In addition, the effects of LPs on SSC were also revealed in our study. Soil erosion and sediment transportation have a similar response to LPs changes, which indicates that it is possible to adjust LPs to mitigate river and reservoir siltation in some special locations. Overall, these results could benefit land use management for better soil and water conservation under the rapid development of southeastern China.

The effects of human activity on the results were not taken into consideration in our study. As mentioned before, construction engineering results in serious soil erosion events [79], and agricultural activity and industrial development consume many water resources [81,82]. A water use dataset should be collected to be used in relevant investigations in the future to reduce the influence of these human activities. In addition, it has been reported that the effects of various LPs on hydrological processes may have discrep-

ancies in different seasons during a year [40,48]. The variations in hydrological processes characteristic in different seasons were not taken into consideration in our study due to the limitations of the hydrological data. A further study should be conducted to clarify these differences. Finally, though the watershed size in our study ranges from 1700 to 80,900 km^2, the number of watersheds used in this study was relatively few. More watersheds with various size should be taken into consideration to obtain more stable correlations between various LMs and hydrological processes.

6. Conclusions

In our study, the relationships between 14 LPs and 4 hydrological indices were investigated for 10 watersheds with various areas in the subtropical monsoon climate zone of southeastern China. The main conclusions are as follows:

(1) From 1990 to 2019, the change trends of WY and RC were not significant for any watersheds, and SEM and SSC decreased in all watersheds except for ZJ, HS, and LX. The main land use conversions were forest land–agricultural land, agricultural land–urban land, and agricultural land–forest land, and urban land expanded drastically in all watersheds. In addition, most LMs changed significantly ($p < 0.05$) for most watersheds, which demonstrates that LPs characteristics changed significantly.

(2) For most watersheds ($\geq$7), WY was negatively correlated with LPI, AI, CONTAG, and COHESION and positively correlated with ED, PAFRAC, DIVISION, LSI, SHDI, SHEI, and MSIEI; RC was negatively correlated with LPI, CONTAG, and COHESION and positively correlated with PAFRAC, DIVISION, SHDI, SHEI, and MSIEI; SEM was negatively correlated with LPI and IJI; SEM and SSC were positively correlated with PAFRAC, NP, PD, COHESION, and MSIEI. In addition, the effects of several LMs (IJI, SHDI, and SHEI) on WY, RC, and SEM had scale effects.

(3) In the subtropical monsoon climate zone, runoff increases when a watershed is dominated by a small patch of landscape. In addition, landscape fragmentation and diversity also increase runoff. Proper landscape fragmentation and physical connectivity would benefit soil erosion and river and reservoir siltation prevention.

More studies should be conducted in various climate zones to enhance the understanding of the relationships between LPs and various hydrological indices, and human activity and seasonal discrepancies should be taken into consideration.

Author Contributions: Conceptualization, C.W.; data curation, Y.M. and W.Z.; formal analysis, X.D., M.L., D.Y. and C.Z.; funding acquisition, X.D., Y.M. and D.Y.; investigation, C.W., W.Z. and M.L.; methodology, C.W.; software, D.Y.; supervision, X.D. and Y.M.; visualization, C.W.; writing—original draft, C.W.; writing—review and editing, X.D., Y.M. and B.S. All authors have read and agreed to the published version of the manuscript.

Funding: This research has been supported by the Second Tibetan Plateau Scientific Expedition and Research Program (STEP, grant number 2019QZKK0103), the European Space Agency (ESA) and National Remote Sensing Center of China (grant number 58516), the Power Construction Corporation of China (grant number DJ-ZDZX-2016-02-09), the Research Fund for Excellent Dissertation of China Three Gorges University (grant number No. 2021BSPY002), and the National Natural Science Foundation of China (grant number No. 52109058).

Data Availability Statement: Not applicable.

Conflicts of Interest: The authors declare no conflict of interest.

Glossary

Abbreviation	Full name	Abbreviation	Full name
LP(s)	Landscape pattern(s)	LMs	Landscape metrics
WY	Water yields	RC	Runoff coefficient
SEM	Soil erosion modulus	SSC	Suspended sediment concentration
SYL	Sediment yields load	*p*	Significance level
NDCA	Number of disjunct core areas	PD	Patch density
LSI	Landscape shape index	SHDI	Shannon's diversity index
DIVISION	Landscape division index	LPI	Largest patch index
COHESION	Patch cohesion index	MSIEI	Modified Simpson's evenness index
AI	Aggregation index	ED	Edge density
PLAND	Percentage of landscape	SWAT	Soil and Water Assessment Tool
InVEST	Integrated Valuation of Ecosystem Services and Trade-offs	WaTEM/SEDEM	Water and Tillage Erosion Model and Sediment Delivery Model
RUSLE	Revised Universal Soil Loss Equation	IUH	Instantaneous Unit Hydrograph
HRUs	Hydrological response units	ZJ	Zhuji
DFK	Dufengkeng	HS	Hushan
LJD	Lijiadu	LX	Lanxi
BL	Boluo	CA	Chaoan
SJ	Shijiao	ZQ	Zhuqi
WZ	Waizhou	masl	Meters above the sea level
DA	Drainage area	AE	Average elevation
PRE	Precipitation	PAFRAC	Perimeter area fractal dimension
NP	Number of patches	IJI	Interspersion and Juxtaposition index
CONTAG	Contiguity index	SHEI	Shannon's evenness index
R	Correlation coefficient		

Appendix A

Table A1. The descriptions of the selected landscape metrics and relevant references.

Categories	Metrics	Definition	Relevant Literature
Edge area	LPI	The ratio of the largest patch to the total landscape area. Unit (%)	[25,31,35,38,50,51]
	ED	The length of the edges per unit area. Unit (Meters/hectare)	[25,38,50,51]
Shape	PAFRAC	An index of patch shape complexity across a wide range of spatial scales.	[25,27,31,35,39,51]
Aggregation	NP	Extent of subdivision or fragmentation of the landscape pattern.	[31,35,38]
	DIVISION	Reflects the degree of fragmentation of the landscape. Unit (Proportion)	[17,35,36]
	AI	Connectivity between patches of landscape types. Unit (%)	[25,31,38,50]
	IJI	The observed interspersion over the maximum possible interspersion for the given number of patch types. Unit (%)	[27,31,39,51]
	CONTAG	An index measuring the extent to which patch types are aggregated or clumped. Unit (%)	[25,31,33,35,38,50,51]
	PD	The number of patches within 1 km^2. Unit (Number per 100 hectares)	[25,31,35,38,50,51]
	LSI	This index reflects the complexity of the boundaries of all patches within the region.	[31,35,50,51]
	COHESION	Measures the physical connectedness of the corresponding patch type.	[25,27,35,38,39,50,51]
Diversity	SHDI	The number of different patch types and the proportional area distribution among patch types.	[25,33,35,38,50,51]
	SHEI	The proportional abundance of each patch type.	[25,27,33,38,39]
	MSIEI	MSIEI equals minus the logarithm of the sum, across all patch types, of the proportional abundance of each patch type squared, which is then divided by the logarithm of the number of patch types.	[25,33]

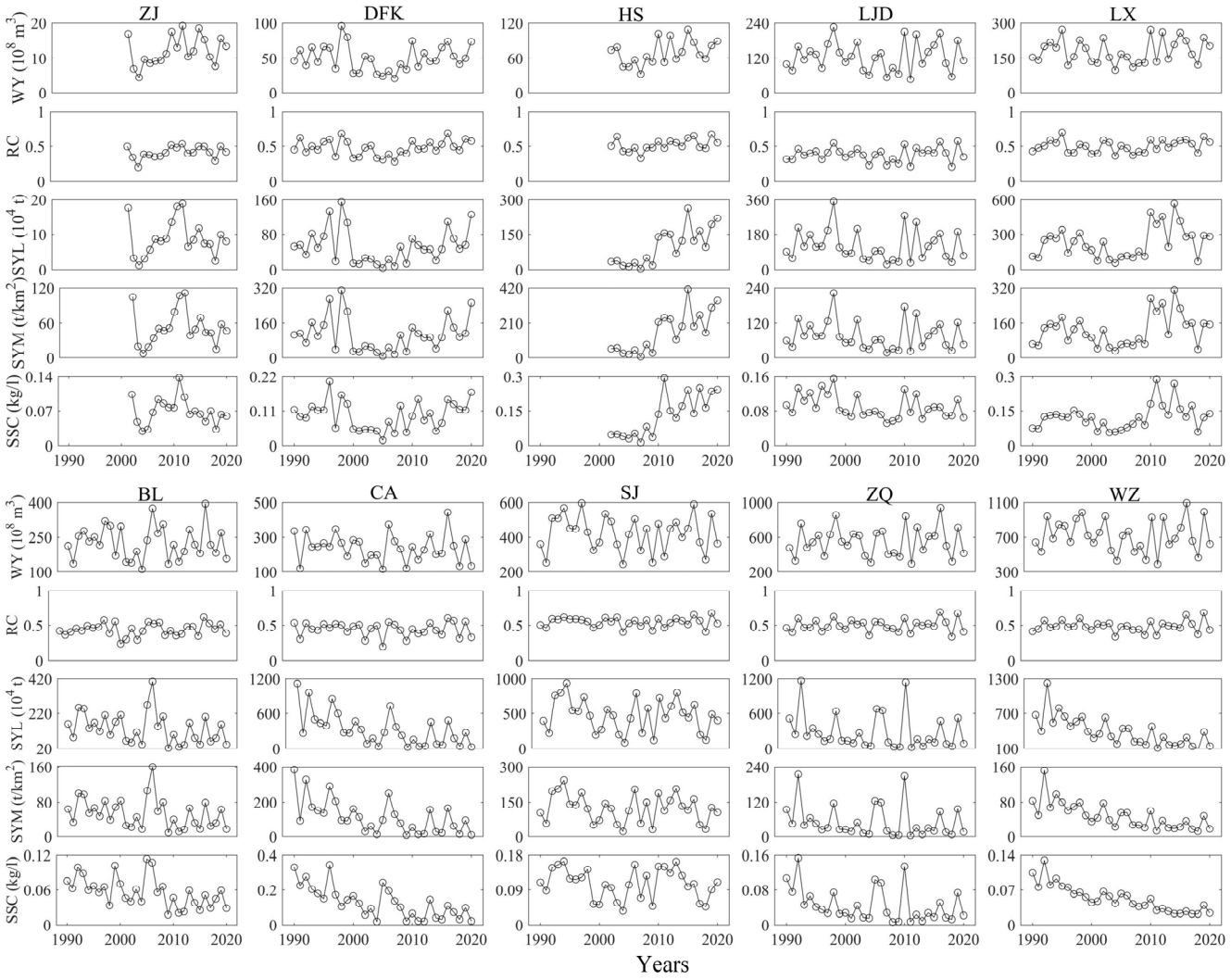

Figure A1. The temporal variations of WY, RC, SYL, SYM, and SSC in the ZJ, DFK, HS, LJD, LX, BL, CA, SJ, ZQ, and WZ watersheds.

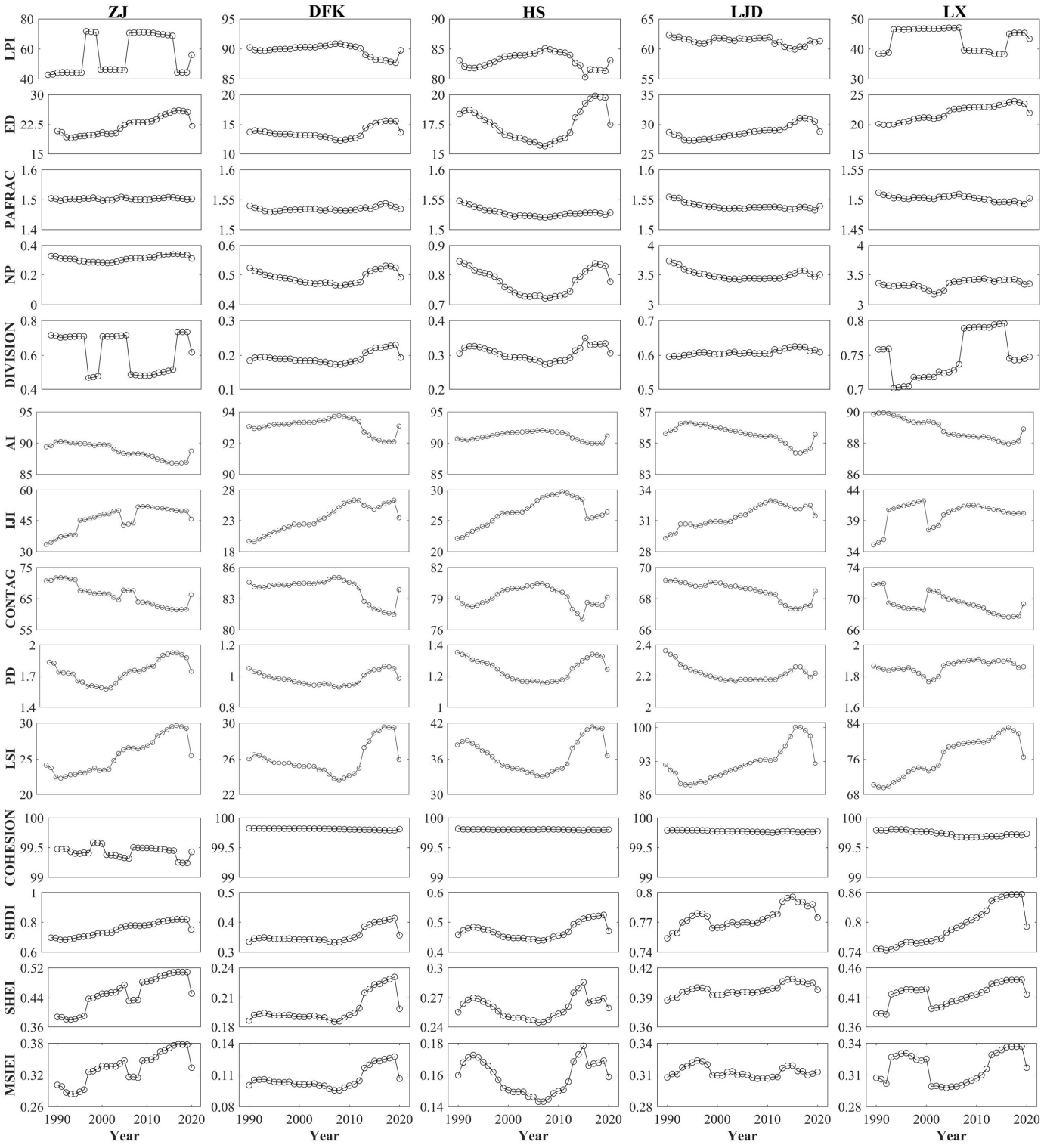

Figure A2. *Cont.*

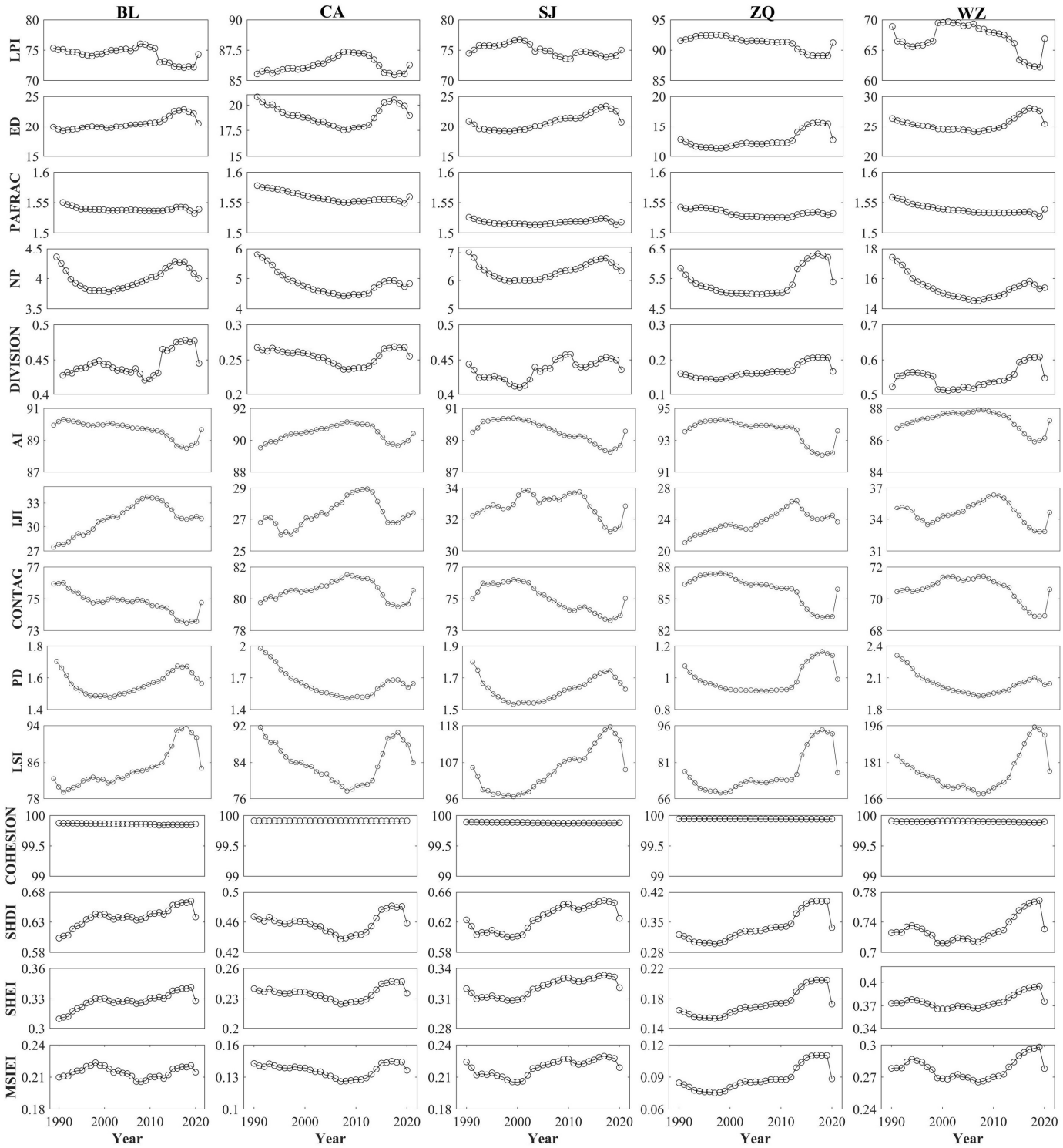

Figure A2. The temporal variations of LPI, ED, PAFRAC, NP, DIVISION, AI, IJI, CONTAG, PD, LSI, COHESION, SHDI, SHEI, and MSIEI in the ZJ, DFK, HS, LJD, LX, BL, CA, SJ, ZQ, and WZ watersheds.

References

1. Rasool, R.; Fayaz, A.; ul Shafiq, M.; Singh, H.; Ahmed, P. Land use land cover change in Kashmir Himalaya: Linking remote sensing with an indicator based DPSIR approach. *Ecol. Indic.* **2021**, *125*, 107447. [CrossRef]
2. Terêncio, D.; Varandas, S.; Fonseca, A.; Cortes, R.; Fernandes, L.; Pacheco, F.; Monteiro, S.; Martinho, J.; Cabral, J.; Santos, J. Integrating ecosystem services into sustainable landscape management: A collaborative approach. *Sci. Total Environ.* **2021**, *794*, 148538. [CrossRef] [PubMed]

3. Nafi'Shehab, Z.; Jamil, N.R.; Aris, A.Z.; Shafie, N.S. Spatial variation impact of landscape patterns and land use on water quality across an urbanized watershed in Bentong, Malaysia. *Ecol. Indic.* **2021**, *122*, 107254. [CrossRef]
4. Devátý, J.; Dostál, T.; Hösl, R.; Krása, J.; Strauss, P. Effects of historical land use and land pattern changes on soil erosion–Case studies from Lower Austria and Central Bohemia. *Land Use Policy* **2019**, *82*, 674–685. [CrossRef]
5. Sahin, V.; Hall, M.J. The effects of afforestation and deforestation on water yields. *J. Hydrol.* **1996**, *178*, 293–309. [CrossRef]
6. Costa, M.H.; Botta, A.; Cardille, J.A. Effects of large-scale changes in land cover on the discharge of the Tocantins River, Southeastern Amazonia. *J. Hydrol.* **2003**, *283*, 206–217. [CrossRef]
7. Kalantari, Z.; Lyon, S.W.; Folkeson, L.; French, H.K.; Stolte, J.; Jansson, P.E.; Sassner, M. Quantifying the hydrological impact of simulated changes in land use on peak discharge in a small catchment. *Sci. Total Environ.* **2014**, *466–467*, 741–754. [CrossRef]
8. Wang, Z.P.; Tian, J.C.; Feng, K.P. Response of runoff towards land use changes in the Yellow River Basin in Ningxia, China. *PLoS ONE* **2022**, *17*, e0265931. [CrossRef]
9. Wei, C.; Dong, X.; Yu, D.; Liu, J.; Reta, G.; Zhao, W.; Kuriqi, A.; Su, B. An alternative to the Grain for Green Program for soil and water conservation in the upper Huaihe River basin, China. *J. Hydrol. Reg. Stud.* **2022**, *43*, 101180. [CrossRef]
10. Molinero-Parejo, R.; Aguilera-Benavente, F.; Gómez-Delgado, M.; Shurupov, N. Combining a land parcel cellular automata (LP-CA) model with participatory approaches in the simulation of disruptive future scenarios of urban land use change. *Comput. Environ. Urban Syst.* **2023**, *99*, 101895. [CrossRef]
11. Liang, X.; Liu, X.; Li, X.; Chen, Y.; Tian, H.; Yao, Y. Delineating multi-scenario urban growth boundaries with a CA-based FLUS model and morphological method. *Landsc. Urban Plan.* **2018**, *177*, 47–63. [CrossRef]
12. Xu, G.; Cheng, Y.; Zhao, C.; Mao, J.; Li, Z.; Jia, L.; Zhang, Y.; Wang, B. Effects of driving factors at multi-spatial scales on seasonal runoff and sediment changes. *Catena* **2023**, *222*, 106867. [CrossRef]
13. Smetanova, A.; Follain, S.; David, M.; Ciampalini, R.; Raclot, D.; Crabit, A.; Le Bissonnais, Y. Landscaping compromises for land degradation neutrality: The case of soil erosion in a Mediterranean agricultural landscape. *J. Environ. Manag.* **2019**, *235*, 282–292. [CrossRef] [PubMed]
14. Lacher, I.L.; Ahmadisharaf, E.; Fergus, C.; Akre, T.; Mcshea, W.J.; Benham, B.L.; Kline, K.S. Scale-dependent impacts of urban and agricultural land use on nutrients, sediment, and runoff. *Sci. Total Environ.* **2019**, *652*, 611–622. [CrossRef] [PubMed]
15. Gonzales-Inca, C.A.; Kalliola, R.; Kirkkala, T.; Lepisto, A. Multiscale Landscape Pattern Affecting on Stream Water Quality in Agricultural Watershed, SW Finland. *Water Resour. Manag.* **2015**, *29*, 1669–1682. [CrossRef]
16. McGarigal, K. *FRAGSTATS: Spatial Pattern Analysis Program for Quantifying Landscape Structure*; US Department of Agriculture, Forest Service, Pacific Northwest Research Station: La Grande, OR, USA, 1995; Volume 351.
17. Bin, L.L.; Xu, K.; Xu, X.Y.; Lian, J.J.; Ma, C. Development of a landscape indicator to evaluate the effect of landscape pattern on surface runoff in the Haihe River Basin. *J. Hydrol.* **2018**, *566*, 546–557. [CrossRef]
18. Shi, P.; Qin, Y.-L.; Li, P.; Li, Z.-B.; Cui, L.-Z. Development of a landscape index to link landscape pattern to runoff and sediment. *J. Mt. Sci.* **2022**, *19*, 2905–2919. [CrossRef]
19. Wang, X.; Liu, X.; Wang, L.; Yang, J.; Wan, X.; Liang, T. A holistic assessment of spatiotemporal variation, driving factors, and risks influencing river water quality in the northeastern Qinghai-Tibet Plateau. *Sci. Total Environ.* **2022**, *851*, 157942. [CrossRef]
20. Stets, E.G.; Sprague, L.A.; Oelsner, G.P.; Johnson, H.M.; Murphy, J.C.; Ryberg, K.; Vecchia, A.V.; Zuellig, R.E.; Falcone, J.A.; Riskin, M.L. Landscape drivers of dynamic change in water quality of US rivers. *Environ. Sci Technol.* **2020**, *54*, 4336–4343. [CrossRef]
21. Liu, Y.; Shen, Y.; Cheng, C.; Yuan, W.; Gao, H.; Guo, P. Analysis of the influence paths of land use and landscape pattern on organic matter decomposition in river ecosystems: Focusing on microbial groups. *Sci. Total Environ.* **2022**, *817*, 153381. [CrossRef]
22. Kumar, G.; Baweja, P.; Gandhi, P.B. Impact of Anthropogenic Activities on Soil Patterns and Diversity. In *Structure and Functions of Pedosphere*; Springer: Berlin/Heidelberg, Germany, 2022; pp. 319–337.
23. Sadeghi, S.H.; Moradi Dashtpagerdi, M.; Moradi Rekabdarkoolai, H.; Schoorl, J.M. Sensitivity analysis of relationships between hydrograph components and landscapes metrics extracted from digital elevation models with different spatial resolutions. *Ecol. Indic.* **2021**, *121*, 107025. [CrossRef]
24. Zhao, X.; Huang, G. Exploring the impact of landscape changes on runoff under climate change and urban development: Implications for landscape ecological engineering in the Yangmei River Basin. *Ecol. Eng.* **2022**, *184*, 106794. [CrossRef]
25. Zhang, S.; Fan, W.; Li, Y.; Yi, Y. The influence of changes in land use and landscape patterns on soil erosion in a watershed. *Sci. Total Environ.* **2017**, *574*, 34–45. [CrossRef] [PubMed]
26. Brini, I.; Alexakis, D.D.; Kalaitzidis, C. Linking Soil Erosion Modeling to Landscape Patterns and Geomorphometry: An Application in Crete, Greece. *Appl. Sci.* **2021**, *11*, 5684. [CrossRef]
27. Zhou, Z.X.; Li, J. The correlation analysis on the landscape pattern index and hydrological processes in the Yanhe watershed, China. *J. Hydrol.* **2015**, *524*, 417–426. [CrossRef]
28. Li, J.; Zhou, Y.; Li, Q.; Yi, S.; Peng, L. Exploring the Effects of Land Use Changes on the Landscape Pattern and Soil Erosion of Western Hubei Province from 2000 to 2020. *Int. J. Environ. Res. Pub. Health* **2022**, *19*, 1571. [CrossRef]
29. Aghsaei, H.; Dinan, N.M.; Moridi, A.; Asadolahi, Z.; Delavar, M.; Fohrer, N.; Wagner, P.D. Effects of dynamic land use/land cover change on water resources and sediment yield in the Anzali wetland catchment, Gilan, Iran. *Sci. Total Environ.* **2020**, *712*, 136449. [CrossRef]
30. Yohannes, H.; Soromessa, T.; Argaw, M.; Dewan, A. Impact of landscape pattern changes on hydrological ecosystem services in the Beressa watershed of the Blue Nile Basin in Ethiopia. *Sci. Total Environ.* **2021**, *793*, 148559. [CrossRef]

31. Chen, C.; Zhao, G.; Zhang, Y.; Bai, Y.; Tian, P.; Mu, X.; Tian, X. Linkages between soil erosion and long-term changes of landscape pattern in a small watershed on the Chinese Loess Plateau. *Catena* **2023**, *220*, 106659. [CrossRef]
32. Wei, C.; Dong, X.; Ma, Y.; Gou, J.; Li, L.; Bo, H.; Yu, D.; Su, B. Applicability comparison of various precipitation products of long-term hydrological simulations and their impact on parameter sensitivity. *J. Hydrol.* **2023**, *618*, 129187. [CrossRef]
33. Ouyang, W.; Skidmore, A.K.; Hao, F.; Wang, T. Soil erosion dynamics response to landscape pattern. *Sci. Total Environ.* **2010**, *408*, 1358–1366. [CrossRef] [PubMed]
34. Xiao, R.; Cao, W.; Liu, Y.; Lu, B. The impacts of landscape patterns spatio-temporal changes on land surface temperature from a multi-scale perspective: A case study of the Yangtze River Delta. *Sci. Total Environ.* **2022**, *821*, 153381. [CrossRef] [PubMed]
35. Yang, Y.Y.; Li, Z.B.; Li, P.; Ren, Z.P.; Gao, H.D.; Wang, T.; Xu, G.C.; Yu, K.X.; Shi, P.; Tang, S.S. Variations in runoff and sediment in watersheds in loess regions with different geomorphologies and their response to landscape patterns. *Environ. Earth Sci.* **2017**, *76*, 517. [CrossRef]
36. Zhang, Y.; Bi, Z.L.; Zhang, X.; Yu, Y. Influence of Landscape Pattern Changes on Runoff and Sediment in the Dali River Watershed on the Loess Plateau of China. *Land* **2019**, *8*, 180. [CrossRef]
37. Gao, F.; He, B.; Xue, S.S.; Li, Y.Z. Impact of landscape pattern change on runoff processes in catchment area of the Ulungur River Basin. *Water Supply* **2020**, *20*, 1046–1058. [CrossRef]
38. Wei, C.; Zhang, Z.; Wang, Z.; Cao, L.; Wei, Y.; Zhang, X.; Zhao, R.; Xiao, L.; Wu, Q. Response of Variation of Water and Sediment to Landscape Pattern in the Dapoling Watershed. *Sustainability* **2022**, *14*, 678. [CrossRef]
39. Li, J.; Zhou, Z.X. Coupled analysis on landscape pattern and hydrological processes in Yanhe watershed of China. *Sci. Total Environ.* **2015**, *505*, 927–938. [CrossRef]
40. Chiang, L.-C.; Wang, Y.-C.; Chen, Y.-K.; Liao, C.-J. Quantification of land use/land cover impacts on stream water quality across Taiwan. *J. Clean Prod.* **2021**, *318*, 128443. [CrossRef]
41. Ke, Q.; Zhang, K. Patterns of runoff and erosion on bare slopes in different climate zones. *Catena* **2021**, *198*, 105069. [CrossRef]
42. Zhu, X.; Li, T.; Tian, Z.; Qu, L.; Liang, Y. Building pedotransfer functions for estimating soil erodibility in southeastern China. *Ecol. Indic.* **2022**, *145*, 109720. [CrossRef]
43. Wei, C.; Dong, X.; Yu, D.; Zhang, T.; Zhao, W.; Ma, Y.; Su, B. Spatio-temporal variations of rainfall erosivity, correlation of climatic indices and influence on human activities in the Huaihe River Basin, China. *Catena* **2022**, *217*, 106486. [CrossRef]
44. Yang, J.; Huang, X. The 30 m annual land cover dataset and its dynamics in China from 1990 to 2019. *Earth Syst. Sci. Data* **2021**, *13*, 3907–3925. [CrossRef]
45. Liang, L.; Yu, L.; Wang, Z. Identifying the dominant impact factors and their contributions to heatwave events over mainland China. *Sci. Total Environ.* **2022**, *848*, 157527. [CrossRef] [PubMed]
46. Wang, L.; Han, X.; Zhang, Y.; Zhang, Q.; Wan, X.; Liang, T.; Song, H.; Bolan, N.; Shaheen, S.M.; White, J.R. Impacts of land uses on spatio-temporal variations of seasonal water quality in a regulated river basin, Huai River, China. *Sci. Total Environ.* **2023**, *857*, 159584. [CrossRef]
47. Lisha, Q.; Qiuan, Z.; Chaofan, Z.; Jiang, Z. Monthly Precipitation Data Set with 1 km Resolution in China from 1960 to 2020[DS/OL]. Science Data Bank: Beijing, China, 2022; Available online: https://cstr.cn/31253.11.sciencedb.01607.CSTR:31253.11.sciencedb.01607 (accessed on 25 December 2022).
48. Xu, S.; Li, S.-L.; Zhong, J.; Li, C. Spatial scale effects of the variable relationships between landscape pattern and water quality: Example from an agricultural karst river basin, Southwestern China. *Agric. Ecosyst. Environ.* **2020**, *300*, 106999. [CrossRef]
49. Han, Y.; Wang, J.-l.; Li, P. Influences of landscape pattern evolution on regional crop water requirements in regions of large-scale agricultural operations. *J. Clean Prod.* **2021**, *327*, 129499. [CrossRef]
50. Jinying, X.; Yang, B.; Hailin, Y.; Xiaowei, W.; Zhifei, M.; Hongwei, Z. Water quality assessment and the influence of landscape metrics at multiple scales in Poyang Lake basin. *Ecol. Indic.* **2022**, *141*, 109096. [CrossRef]
51. Shi, Z.H.; Ai, L.; Li, X.; Huang, X.D.; Wu, G.L.; Liao, W. Partial least-squares regression for linking land-cover patterns to soil erosion and sediment yield in watersheds. *J. Hydrol.* **2013**, *498*, 165–176. [CrossRef]
52. Machado, R.E.; Cardoso, T.O.; Mortene, M.H. Determination of runoff coefficient (C) in catchments based on analysis of precipitation and flow events. *Int. Soil Water Conserv. Res.* **2022**, *10*, 208–216. [CrossRef]
53. Romano, G.; Abdelwahab, O.M.; Gentile, F. Modeling land use changes and their impact on sediment load in a Mediterranean watershed. *Catena* **2018**, *163*, 342–353. [CrossRef]
54. Wu, L.; Yao, W.W.; Ma, X.Y. Using the comprehensive governance degree to calibrate a piecewise sediment delivery ratio algorithm for dynamic sediment predictions: A case study in an ecological restoration watershed of northwest China. *J. Hydrol.* **2018**, *564*, 888–899. [CrossRef]
55. Wang, J.; Shi, B.; Zhao, E.; Yuan, Q.; Chen, X. The long-term spatial and temporal variations of sediment loads and their causes of the Yellow River Basin. *Catena* **2022**, *209*, 105850. [CrossRef]
56. Weisberg, S. *Applied Linear Regression*; John Wiley & Sons: Hoboken, NJ, USA, 2005; Volume 528.
57. Parhizkar, M.; Shabanpour, M.; Lucas-Borja, M.E.; Zema, D.A. Variability of rill detachment capacity with sediment size, water depth and soil slope in forest soils: A flume experiment. *J. Hydrol.* **2021**, *601*, 126625. [CrossRef]
58. Dall'Agnol, R.; Sahoo, P.K.; Salomao, G.N.; de Araujo, A.D.M.; da Silva, M.S.; Powell, M.A.; Ferreira, J.; Ramos, S.J.; Martins, G.C.; da Costa, M.F.; et al. Soil-sediment linkage and trace element contamination in forested/deforested areas of the Itacaiunas River Watershed, Brazil: To what extent land-use change plays a role? *Sci. Total Environ.* **2022**, *828*, 154327. [CrossRef] [PubMed]

59. Tiku, M. Tables of the power of the F-test. *J. Am. Stat. Assoc.* **1967**, *62*, 525–539. [CrossRef]
60. Meals, D.W.; Dressing, S.A.; Davenport, T.E. Lag Time in Water Quality Response to Best Management Practices: A Review. *J. Environ. Qual.* **2010**, *39*, 85–96. [CrossRef]
61. Li, Y.; Li, Y.R.; Fang, B.; Wang, Q.Y.; Chen, Z.F. Impacts of ecological programs on land use and ecosystem services since the 1980s: A case-study of a typical catchment on the Loess Plateau, China. *Land Degrad. Dev.* **2022**, *33*, 3271–3282. [CrossRef]
62. Fenicia, F.; McDonnell, J.J. Modeling streamflow variability at the regional scale: (1) perceptual model development through signature analysis. *J. Hydrol.* **2022**, *605*, 127287. [CrossRef]
63. Schilling, K.E.; Wolter, C.F. A GIS-based groundwater travel time model to evaluate stream nitrate concentration reductions from land use change. *Environ. Geol.* **2007**, *53*, 433–443. [CrossRef]
64. Barlow, K.M.; Weeks, A.; Christy, B. Modelling the response in streamflow to increased forestry plantations. In Proceedings of the 20th International Congress on Modelling and Simulation (MODSIM), Adelaide, Australia, 1–6 December 2013; pp. 538–544.
65. He, D.; Chen, Z.; Zhou, J.; Yang, T.; Lu, L. The Heterogeneous Impact of High-Speed Railway on Urban Expansion in China. *Remote Sens.* **2021**, *13*, 4914. [CrossRef]
66. Mostafa, E.; Li, X.; Sadek, M.; Dossou, J.F. Monitoring and Forecasting of Urban Expansion Using Machine Learning-Based Techniques and Remotely Sensed Data: A Case Study of Gharbia Governorate, Egypt. *Remote Sens.* **2021**, *13*, 4498. [CrossRef]
67. Sarkodie, S.A.; Owusu, P.A. Global land-use intensity and anthropogenic emissions exhibit symbiotic and explosive behavior. *Iscience* **2022**, *25*, 104741. [CrossRef] [PubMed]
68. Shi, P.; Zhang, Y.; Ren, Z.; Yu, Y.; Li, P.; Gong, J. Land-use changes and check dams reducing runoff and sediment yield on the Loess Plateau of China. *Sci. Total Environ.* **2019**, *664*, 984–994. [CrossRef] [PubMed]
69. Dong, H.; Song, Y.; Chen, L.; Liu, H.; Fu, X.; Xie, M. Soil erosion and human activities over the last 60 years revealed by magnetism, particle size and minerals of check dams sediments on the Chinese Loess Plateau. *Environ. Earth Sci.* **2022**, *81*, 162. [CrossRef]
70. Fan, J.; Xu, Y.; Ge, H.; Yang, W. Vegetation growth variation in relation to topography in Horqin Sandy Land. *Ecol. Indic.* **2020**, *113*, 106215. [CrossRef]
71. Zhang, Z.D.; Chen, S.J.; Wan, L.W.; Cao, J.; Zhang, Q.; Yang, C.X. The effects of landscape pattern evolution on runoff and sediment based on SWAT model. *Environ. Earth Sci.* **2021**, *80*, 2. [CrossRef]
72. Deng, Y.; Wu, S.; Ke, J.; Zhu, A. Effects of meteorological factors and groundwater depths on plant sap flow velocities in karst critical zone. *Sci. Total Environ.* **2021**, *781*, 146764. [CrossRef]
73. Yang, M.; Li, X.Z.; Hu, Y.M.; He, X.Y. Assessing effects of landscape pattern on sediment yield using sediment delivery distributed model and a landscape indicator. *Ecol. Indic.* **2012**, *22*, 38–52. [CrossRef]
74. Ma, B.; Wu, C.; Ding, F.; Zhou, Z. Predicting basin water quality using source-sink landscape distribution metrics in the Danjiangkou Reservoir of China. *Ecol. Indic.* **2021**, *127*, 107697. [CrossRef]
75. Ouyang, W.; Wu, Y.; Hao, Z.; Zhang, Q.; Bu, Q.; Gao, X. Combined impacts of land use and soil property changes on soil erosion in a mollisol area under long-term agricultural development. *Sci. Total Environ.* **2018**, *613*, 798–809. [CrossRef]
76. de Carvalho, D.F.; Macedo, P.M.S.; Pinto, M.F.; de Almeida, W.S.; Schultz, N. Soil loss and runoff obtained with customized precipitation patterns simulated by InfiAsper. *Int. Soil Water Conserv. Res.* **2022**, *10*, 407–413. [CrossRef]
77. Pijl, A.; Reuter, L.E.; Quarella, E.; Vogel, T.A.; Tarolli, P. GIS-based soil erosion modelling under various steep-slope vineyard practices. *Catena* **2020**, *193*, 104604. [CrossRef]
78. Zhu, X.; Liang, Y.; Tian, Z.; Wang, X. Analysis of scale-specific factors controlling soil erodibility in southeastern China using multivariate empirical mode decomposition. *Catena* **2021**, *199*, 105131. [CrossRef]
79. Wallace, M.; Mickovski, S.B.; Griffin, I. An innovative framework for selecting sustainable options to reduce the risk of soil erosion and environmental pollution incidents on road construction sites. In Proceedings of the XVII ECSMGE-2019: Geotechnical Engineering Foundation of the Future, Reykjavik, Iceland, 1–6 September 2019; The Icelandic Geotechnical Society: Reykjavik, Iceland, 2019.
80. Zhang, Y.F.; Wang, N.; Tang, C.J.; Zhang, S.Q.; Song, Y.J.; Liao, K.T.; Nie, X.F. A New Indicator to Better Represent the Impact of Landscape Pattern Change on Basin Soil Erosion and Sediment Yield in the Upper Reach of Ganjiang, China. *Land* **2021**, *10*, 990. [CrossRef]
81. Rufí-Salís, M.; Petit-Boix, A.; Villalba, G.; Sanjuan-Delmás, D.; Parada, F.; Ercilla-Montserrat, M.; Arcas-Pilz, V.; Munoz-Liesa, J.; Rieradevall, J.; Gabarrell, X. Recirculating water and nutrients in urban agriculture: An opportunity towards environmental sustainability and water use efficiency? *J. Clean Prod.* **2020**, *261*, 121213. [CrossRef]
82. Trang, T.T.; Bush, S.R.; van Leeuwen, J. Enhancing institutional capacity in a centralized state: The case of industrial water use efficiency in Vietnam. *J. Ind. Ecol.* **2022**, *27*, 210–222. [CrossRef]